GE Nuclear Energy

Technical Services Business
General Electric Company,
175 Curtner Avenue, San Jose, CA 95125

GE-NE-523-A164-1294
DRF 137-0010-7
April 1995

HOPE CREEK 1 GENERATING STATION RPV SURVEILLANCE MATERIALS TESTING AND FRACTURE TOUGHNESS ANALYSIS

Prepared by: R.G. Carey
R. G. Carey, Engineer
Engineering Services

Verified by: B J Branlund
B. J. Branlund, Principal Engineer
RPV Integrity

Approved by: T A Caine
T. A. Caine, Principal Engineer
Reactor Internals Management

**IMPORTANT NOTICE REGARDING
CONTENTS OF THIS REPORT
PLEASE READ CAREFULLY**

This report was prepared by General Electric solely for the use of Public Service Electric & Gas Company. The information contained in this report is believed by General Electric to be an accurate and true representation of the facts known, obtained or provided to General Electric at the time this report was prepared.

The only undertakings of the General Electric Company respecting information in this document are contained in the contract between the customer and General Electric Company, as identified in the purchase order for this report and nothing contained in this document shall be construed as changing the contract. The use of this information by anyone other than the customer or for any purpose other than that for which it is intended, is not authorized; and with respect to any unauthorized use, General Electric Company makes no representation or warranty, and assumes no liability as to the completeness, accuracy, or usefulness of the information contained in this document.

CONTENTS

CONTENTS

APPENDICES

TABLES

ILLUSTRATIONS

ILLUSTRATIONS (continued)

ABSTRACT

The surveillance capsule at 30° azimuth location was removed from the Hope Creek 1 reactor in Spring 1994. The capsule contained flux wires for neutron fluence measurement and Charpy and tensile test specimens for material property evaluation. The flux wires were evaluated to determine the fluence experienced by the test specimens. Charpy V-Notch impact testing and uniaxial tensile testing were performed to establish the properties of the irradiated surveillance materials. Unirradiated Charpy and tensile specimens were tested as well to obtain the appropriate baseline data.

The irradiated Charpy data for the plate and weld specimens were compared to the unirradiated data to determine the shift in Charpy curves due to irradiation. The results are within the predictions of the Regulatory Guide 1.99 Revision 2.

The irradiated tensile data for the plate and weld specimens were compared to the unirradiated data to determine the effect of irradiation on the stress-strain relationship of the materials. The majority of the changes shown in the materials were consistent with the irradiation embrittlement effects shown by the Charpy specimens.

The flux wire results, combined with the lead factor determined from the last fuel cycle, were used to estimate the 32 EFPY fluence. The resulting estimate was about 14% greater than the previous estimate of nominal 32 EFPY fluence; therefore, new pressure-temperature curves were generated.

ACKNOWLEDGMENTS

The author gratefully acknowledges the efforts of other people towards completion of the contents of this report.

Charpy testing was completed by G. P. Wozadlo and G. E. Dunning. Tensile specimen testing was done by S. B. Wisner and G. E. Dunning, and chemical composition analysis was performed by P. C. Wall and R. D. Reager. Flux wire testing was performed by R. Kruger and R. D. Reager.

1. INTRODUCTION

Part of the effort to assure reactor vessel integrity involves evaluation of the fracture toughness of the vessel ferritic materials. The key values which characterize a material's fracture toughness are the reference temperature of nil-ductility transition (RT_{NDT}) and the upper shelf energy (USE). These are defined in 10CFR50 Appendix G [1] and in Appendix G of the ASME Boiler and Pressure Vessel Code, Section XI [2]. These documents contain requirements used to establish the pressure- temperature operating limits which must be met to avoid brittle fracture.

Appendix H of 10CFR50 [3] and ASTM E185-66 [4] establish the design requirements to be met for surveillance of the Hope Creek 1 reactor vessel materials. Capsule removal and testing were done per the requirements of ASME E185-82 [6] to the extent practical. The first vessel surveillance specimen capsule required by 10CFR50 Appendix H [3] was removed in Spring 1994. The irradiated capsule was sent to the GE Vallecitos Nuclear Center (VNC) for testing. The surveillance capsule contained flux wires for neutron flux monitoring and Charpy V-Notch impact test specimens and uniaxial tensile test specimens fabricated using materials from the vessel materials within the core beltline region. The impact and tensile specimens were tested to establish properties for the irradiated materials. Unirradiated tensile specimens were sent from site to GE Nuclear Energy (GE-NE) in San Jose and tested using similar testing procedures.

The results of the surveillance specimen testing are presented in this report, as required by 10CFR50 Appendices G and H [1 & 3]. The irradiated material properties are compared to the unirradiated properties to determine the effect of irradiation on the tensile properties, through tensile testing, and on material toughness, through Charpy testing. Flux wire results and updated lead factor analyses are used to determine the need for changes to the pressure-temperature (P-T) curves.

2. SUMMARY AND CONCLUSIONS

2.1 SUMMARY OF RESULTS

The 30° azimuth surveillance capsule was removed and shipped to VNC. The flux wires, Charpy V-Notch and tensile test specimens removed from the capsule were tested according to ASTM E185-82 [6]. The methods and results of the testing are presented as follows:

a. Section 3: Surveillance Program Background

b. Section 4: Peak RPV Fluence Evaluation

b. Section 5: Charpy V-Notch Impact Testing

c. Section 6: Tensile Testing

d. Section 7: Development of Operating Limits Curves

The significant results of the evaluation are below:

a. The 30° azimuth position capsule was removed from the reactor. The capsule contained 9 flux wires: 3 copper (Cu), 3 iron (Fe), and 3 nickel (Ni). There were 36 Charpy V-Notch specimens in the capsule: 12 each of plate material, weld material, and heat affected zone (HAZ) material. The 6 tensile specimens removed consisted of 2 plate, 2 weld, and 2 HAZ metal specimens.

b. The chemical compositions of copper (Cu) and nickel (Ni) for the irradiated surveillance materials were analyzed (see Table 3-3). The values for the irradiated surveillance plate are 0.09% Cu and 0.66% Ni. The values for the irradiated surveillance weld are 0.06% Cu and 0.46% Ni.

c. The purpose of the flux wire testing was to determine the neutron flux at the surveillance capsule location. The flux wire results show that the fluence (from E>1 MeV flux) received by the surveillance specimens for 6.01 EFPY was 1.42×10^{17} n/cm^2 at removal (see Section 4.3).

d. A neutron transport computation was performed, based on the performance of the last fuel cycle. Relative flux distributions in the azimuthal and axial directions were developed. The lead factor relating the surveillance capsule flux to the peak inside surface flux was 1.01 (see Section 4.2.2).

e. The surveillance Charpy V-Notch specimens were impact tested at temperatures selected to define the transition of the fracture toughness curves of the plate, weld, and HAZ materials. Measurements were taken of absorbed energy, lateral expansion and percentage shear. From absorbed energy and lateral expansion curve-fit results (for plate and weld metal only), the values of USE and of index temperature for 30 ft-lb, 50 ft-lb and 35 mils lateral expansion (MLE) were obtained (see Table 5-4). Fracture surface photographs of each specimen are presented in Appendix A.

f. The curves of irradiated Charpy specimens and unirradiated Charpy specimens established the 30 ft-lb index temperature irradiation shift. The plate material showed a measured shift of 4°F and the weld material showed a measured shift of 61°F. The measured shifts for the plate and for the weld (for a fluence of 1.42×10^{17} n/cm^2) were within their respective Reg. Guide 1.99 [7] range predictions ($\Delta RT_{NDT} \pm 2\sigma$) of -26°F to 42°F and -41°F to 71°F, respectively (see Section 5.4.1).

g. The measured decrease in USE of 14% for the plate material compares to a Reg. Guide 1.99 prediction of 7%. The measured decrease in USE of 5% for the weld material compares to a Reg. Guide 1.99 prediction of 8.5% (see Section 5.4.2).

h. The irradiated tensile specimens were tested at room temperature (70°F), and reactor operating temperature (550°F). The results in comparison to unirradiated data were tabulated (see Tables 6-3 and 6-4) for each specimen including yield and ultimate tensile strength, uniform and total elongation, and reduction of area. The results generally showed increasing strength and decreasing ductility, consistent with expectations for irradiation embrittlement.

i. The 32 EFPY peak vessel inside surface fluence prediction is 7.5×10^{17} n/cm^2, based on the flux wire test and lead factor results (see Section 4.3). This is about 14% greater than the previously determined nominal value (6.6×10^{17} n/cm^2) using the first cycle dosimetry [11].

j. As a part of the development of the pressure-temperature (P-T) operating limits curves, the adjusted reference temperature (ART = initial RT_{NDT} + ΔRT_{NDT} + Margin) was predicted for each beltline material, based on the methods of Reg. Guide 1.99. The ART for the limiting material, plate heat 5K3025/1, at 32 EFPY is 72.5°F.

k. The beltline material USE values at 32 EFPY were predicted using the methods of Reg. Guide 1.99, with initial beltline USE values based on estimated USE values for the plates and 10°F test results for the welds (see Table 7-3). It is expected that the actual 32 EFPY USE will be in excess of 50 ft-lbs for all beltline plates and welds. In addition, the results of the USE testing for the surveillance materials show that the BWROG Equivalent Margin Analysis is bounding.

l. P-T curves were developed for three reactor conditions: pressure test (Curve A), non-nuclear heatup and cooldown (Curve B), and core critical operation (Curve C). The P-T curves, shown in Figures 7-1, 2, and 3, are valid for 32 EFPY of operation.

2.2 CONCLUSIONS

The requirements of 10CFR50 Appendix G [1] deal basically with vessel design life conditions and with limits of operation designed to prevent brittle fracture. Based on the evaluation of surveillance testing results, and the associated analyses, the following conclusions are made:

a. The measured 30 ft-lb shifts are within the Regulatory Guide 1.99, Revision 2 predictions, as is the measured USE decrease for the surveillance weld. The measured USE decrease for the surveillance plate was greater than predicted.

b. The values of ART and USE for the reactor vessel beltline materials are shown by calculation to remain within limits in 10CFR50 Appendix G [1] for at least 32 EFPY of operation.

3. SURVEILLANCE PROGRAM BACKGROUND

3.1 CAPSULE RECOVERY

The reactor pressure vessel (RPV) surveillance program consist of three surveillance capsules at the 30°, 120°, and 300° azimuths at the core midplane. The specimen capsules are held against the RPV inside surface by a spring loaded specimen holder. Each capsule is located at a similar positions relative to the core geometry because of core symmetry; therefore, each capsule is expected to receive equal irradiation. During the Spring 1994 outage, the 30° positioned capsule was removed. The capsule was cut from its holder assembly and shipped by cask to the GE Vallecitos Nuclear Center (VNC), where testing was performed.

Upon arrival at VNC, the capsule basket was examined for identification. The Hope Creek 1 reactor code number is 57, as specified in GE drawing 105D4714. The holder part number 131C7717G6 as specified in GE drawing 105D4719G7 from master parts list 238X111AC was stamped on the basket and provided positive identification as the 30° surveillance capsule materials for Hope Creek 1. The general condition of the basket as received is shown in Figure 3-1. The basket contained three impact (Charpy) specimen capsules and three tensile specimen capsules. Each tensile specimen capsule contained two tensile specimens. Each Charpy specimen capsule contained 12 plate, weld, or HAZ Charpy specimens and 3 flux wires (one iron, one copper, and one nickel) in a sealed helium environment.

3.2 RPV MATERIALS AND FABRICATION BACKGROUND

3.2.1 Fabrication History

The Hope Creek 1 RPV is a 251 inch diameter BWR/4 design. Construction was performed by Babcock-Hitachi to the Winter 1968 edition of the ASME Code Section III with Winter 1969 Addenda. The shell and head plate materials are ASME SA533, Grade B, Class 1 low alloy steel (LAS). The nozzles and closure flanges are ASME SA508 Class 2 LAS, and the closure flange bolting materials are ASME SA540 Grade B24 LAS. The plates and welds in the beltline region of the RPV are shown in Figure 3-2. The vessel plates were heat treated prior to welding: austenitized typically at 1580°F-1635°F for approximately 3.5 hours and tempered typically at 1200°F-1256°F for approximately 3.5 hours. The post weld heat treat was typically 40.5 hours minimum at temperatures between 1100°F-1130°F. Submerged arc or shielded metal

arc welding of plates was followed by post weld heat treatment typically at 1112°F-1170°F for at least 40 hours.

3.2.2 Material Properties of RPV at Fabrication

The chemical and mechanical properties of the vessel materials were retrieved from information documented in the response to Generic Letter 92-01 [15], the UFSAR [5] and the Tech .Spec. [9]. Table 3-1 shows the chemistry data for the beltline materials. Properties of the beltline materials and other locations of interest are presented in Table 3-2.

3.2.3 Specimen Chemical Composition

Samples were taken from the irradiated surveillance plate and weld tensile specimens after they were tested. Chemical analyses were performed using a Spectraspan III plasma emission spectrometer. Each sample was etched then dissolved in an acid solution to a specific concentration for each gram of metal. The spectrometer was calibrated for determination of Mn, Ni, Mo, and Cu by diluting National Institute of Standards and Technology (NIST) Spectrometric Standard Solutions. The phosphorus calibration involved analysis of four reference materials from NIST with known phosphorus levels. Analysis accuracies are $\pm$0.005% (absolute) of reported value for phosphorus and $\pm$5% (relative) of reported value for other elements. The chemical composition results are given in Table 3-3 for irradiated surveillance plate and weld materials. The results show good agreement with corresponding unirradiated surveillance plate data, but the corresponding unirradiated surveillance weld data have higher %Wt content for most elements.

3.3 SPECIMEN DESCRIPTION

The surveillance capsule holder contained 36 Charpy specimens: base metal (12), weld metal (12), and HAZ (12). There were 6 tensile specimens: base metal (2), weld metal (2), and HAZ (2). The holder contained 9 flux wires: 3 iron, 3 nickel and 3 copper. The chemistry and fabrication history for the Charpy and tensile specimens are described in this section. All materials used for surveillance were beltline materials.

3.3.1 Charpy Specimens

The fabrication of the Charpy specimens is described in the Babcock-Hitachi drawing [8] on the surveillance test program.

The base metal specimens were cut from Heat 5K3238/1. The test plates received a similar heat treatment as the fabrication plates for Heat 5K3238/1 per requirement of GE document 21A8707 [16], including the post weld heat treatment. Specimens were machined from the 1/4 T and 3/4 T positions in the plate, in the longitudinal orientation (long axis parallel to the rolling direction) to the dimensions in GE drawing 158B7977. The base metal Charpy specimens from the surveillance capsule were stamped on one end with the reactor number, 57, and on the other end with "P1", which designates base metal.

The weld metal and HAZ Charpy specimens were fabricated from two pieces of the surveillance test plate Heat 5K3238/1 are welded together with a weld which was specified to be identical to the beltline longitudinal seam welds. The general welding spec. used was RS G576 and the proc. qual. test spec. no. was RS 9551. Actual welding records obtained from Babcock-Hitachi show the surveillance weld to be submerged arc welding Heat/Lot D53040/1125-02205, except at the root of the weld. However, weld metal specimens were fabricated away from the root of the weld. This heat and lot number is the same as that of a beltline weld. The welded test plate for the weld and HAZ Charpy specimens received a similar post weld heat treatment as the vessel material, per GE doucment 21A8707 [16]. The base metal orientation in the weld and HAZ specimens was longitudinal. The specimens were machined to the dimensions in GE drawing 158B7977 and stamped on one end with the reactor number and on the other with "P3" for weld metal or "P4" for HAZ.

3.3.2 Tensile Specimens

Fabrication of the surveillance tensile specimens is also described in the Babcock-Hitachi surveillance specimen drawings [8]; the specimens are machined to the dimensions in GE drawing 166B7062. The materials, and thus the chemical compositions and heat treatments for the base, weld, and HAZ tensiles are the same as those for the corresponding Charpy specimens. The identifications of the base, weld, and HAZ tensile specimens are: reactor number 57 on one end and P1, P2, or P3 on the other end.

The base metal specimens were machined from material at the 1/4 T and 3/4 T depth. The specimens were oriented along the plate rolling direction. The gage section was tapered to a minimum ∅ 0.250 inch at the center. The weld specimens were machined entirely from weld metal, scrapping material that might include base metal. The HAZ specimen blanks were cut from the welded test plates such that the gage section minimum diameters were machined at the weld fusion line. The finished HAZ specimens are approximately half weld metal and half base metal oriented along the plate rolling direction.

Table 3-1
CHEMICAL COMPOSITION OF RPV BELTLINE MATERIALS

Identification	Heat No.	C	Mn	P	S	Si	Ni	Mo	Cu
		Composition by Weight Percent							
Lower Plates:	6C45/1	0.18	1.49	0.008	0.010	0.31	0.57	0.50	0.08
Shell Course No. 5	6C35/1	0.20	1.46	0.010	0.011	0.27	0.54	0.51	0.09
	5K3230/1	0.19	1.44	0.010	0.012	0.30	0.56	0.50	0.07
Lower-Intermediate	5K2963/1	0.22	1.43	0.009	0.008	0.29	0.58	0.59	0.07
Plates:	5K2530/1	0.20	1.43	0.010	0.008	0.30	0.56	0.54	0.08
Shell Course No. 4	5K3238/1	0.20	1.45	0.012	0.008	0.31	0.63	0.56	0.09
Intermediate Plates	5K2698/1	0.21	1.41	0.010	0.010	0.30	0.58	0.56	0.10
Shell Course No. 3	5K2608/1	0.19	1.46	0.009	0.014	0.30	0.58	0.53	0.09
	5K3025/1	0.17	1.46	0.012	0.009	0.30	0.71	0.52	0.15
Surveillance Plate:	5K3238/1	0.20	1.42	0.012	0.012	0.29	0.62	0.54	0.09
Welds:	510-01205	0.072	1.2	0.01	0.011	0.42	0.54	0.45	0.09
	519-01205	0.051	1.17	0.01	0.007	0.26	0.53	0.45	0.01
	504-01205	0.06	1.3	0.011	0.005	0.26	0.51	0.41	0.01
	001-01205	0.058	1.26	0.012	0.006	0.25	0.51	0.40	0.02
	D53040 (Flux 1810-02205)	0.088	1.69	0.012	0.003	0.34	0.68	0.45	0.10
	D53040 (Flux 1125-02205)	0.01	1.68	0.01	0.004	0.3	0.63	0.43	0.08
	D55733 (Flux 1810-02205)	0.076	1.57	0.013	0.003	0.34	0.68	0.43	0.1
Surveillance Weld:	D53040 (Flux 1125-02205)	0.11	1.69	0.012	0.005	0.31	0.68	0.51	0.09

Table 3-2

MECHANICAL PROPERTIES OF BELTLINE AND OTHER SELECTED RPV MATERIALS

Location	Heat Number	Initial RTndt (°F)
Beltline [a]:		
Lower Plates	5K3230/1	-10
(Shell Course No. 5)	6C35/1	-11
	6C45/1	1
Lower Intermediate Plates	5K2963/1	-10
(Shell Course No. 4)	5K2530/1	19
	5K3238/1	7
Intermediate Plates	5K3025/1	19
(Shell Course No. 3)	5K2608/1	19
	5K2698/1	19
LPCI Nozzle	19468/1	-20
	10024/1	-20
Welds	001-01205	-40
	510-01205	-40
	D53040/1125-02205	-30
	519-01205	-49
	504-01205	-31
	D55733/1810-02205	-40
	D53040/1810-02205	-49
Non-Beltline [b]:		
Vessel Flange		10
Top Head Flange		10
Top Head Torus		19
Feedwater Nozzle		-20
Shell Ring Connected to Vessel Flange		19
Bottom Head Dome		30
Bottom Head Torus		30
Closure Studs		met 45 ft-lb and 25 mils @10°F

[a] Test data information from UFSAR [5]

[b] Test data information from Tech. Spec. [9]

Table 3-3

CHEMICAL COMPOSITION OF IRRADIATED AND UNIRRADIATED SURVEILLANCE SPECIMENS

Identification	Mn	P	Cr	Ni	Mo	Cu
	Composition by Weight Percent					
PLATE:						
Tensile P1A (RT°F)	1.31	0.011	0.14	0.62	0.54	0.08
Tensile P1B (550°F)	1.34	0.011	0.10	0.70	0.58	0.09
Average Tensile				0.66		0.09
Beltline Plate [a] 5K3238/1	1.45	0.012	--	0.63	0.56	0.09
Surveillance Plate [b] 5K3238/1	1.42	0.012	--	0.62	0.54	0.09
Average Plate Chemistry [c]				**0.64**		**0.09**
WELD:						
Tensile P2A (RT°F)	1.13	0.016	0.10	0.41	0.30	0.05
Tensile P2B (550°F)	1.41	0.017	0.12	0.50	0.34	0.06
Average Tensile				0.46		0.06
Beltline Weld [a] D53040, Flux 1125-02205	1.68	0.010	--	0.63	0.43	0.08
Surveillance Weld [b] D53040, Flux 1125-02205	1.69	0.012	--	0.68	0.51	0.09
Average Weld Chemistry [c]				**0.59**		**0.08**

[a] Beltline specimen data from Table 3-1 has been added for comparison

[b] Unirradiated surveillance material from Table 3-1

[c] Average chemistry = (Average Tensile + Beltline + Surveillance)/3

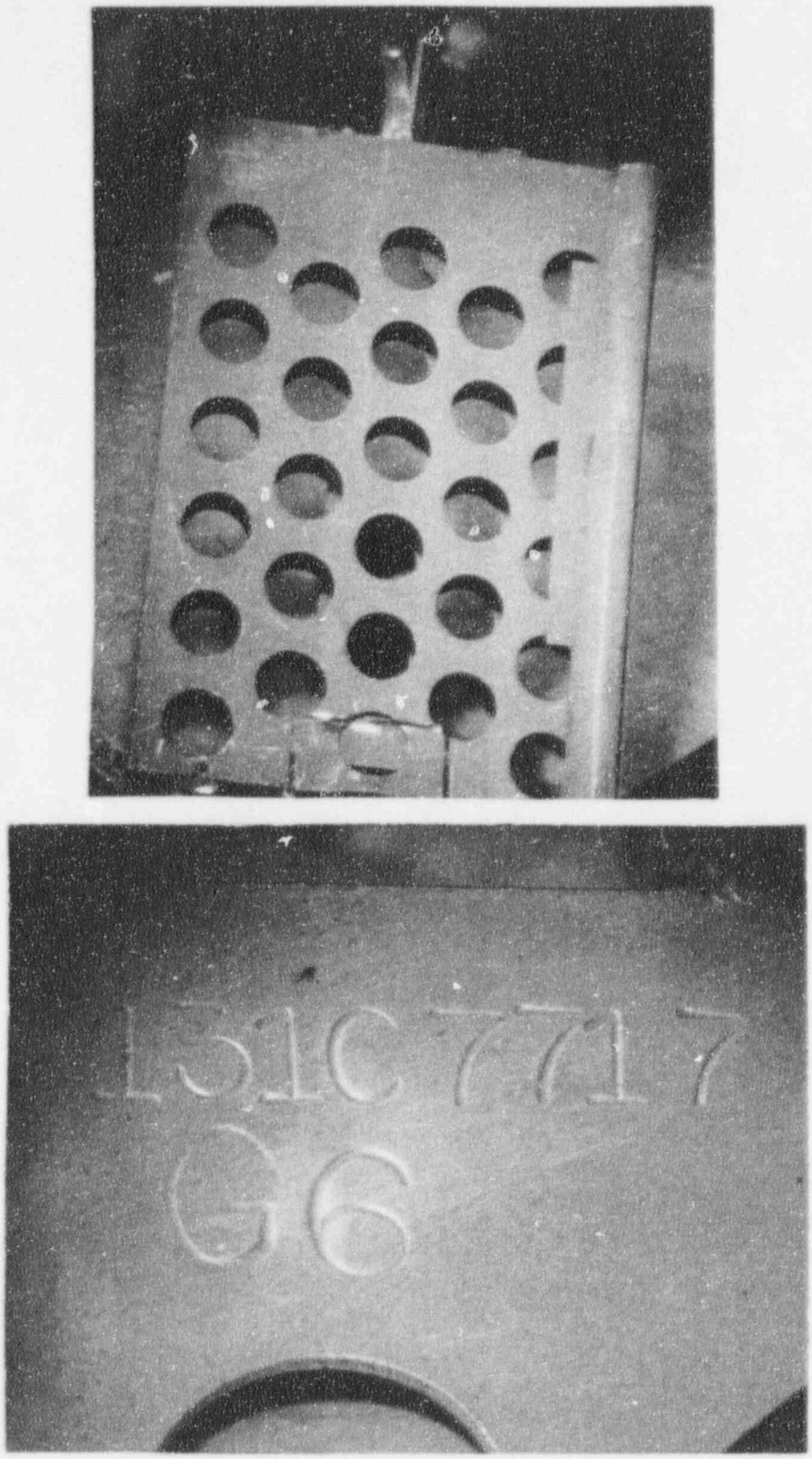

Figure 3-1. Surveillance Capsule Holder Recovered From Hope Creek
(Holder marked as "131C7717G6)

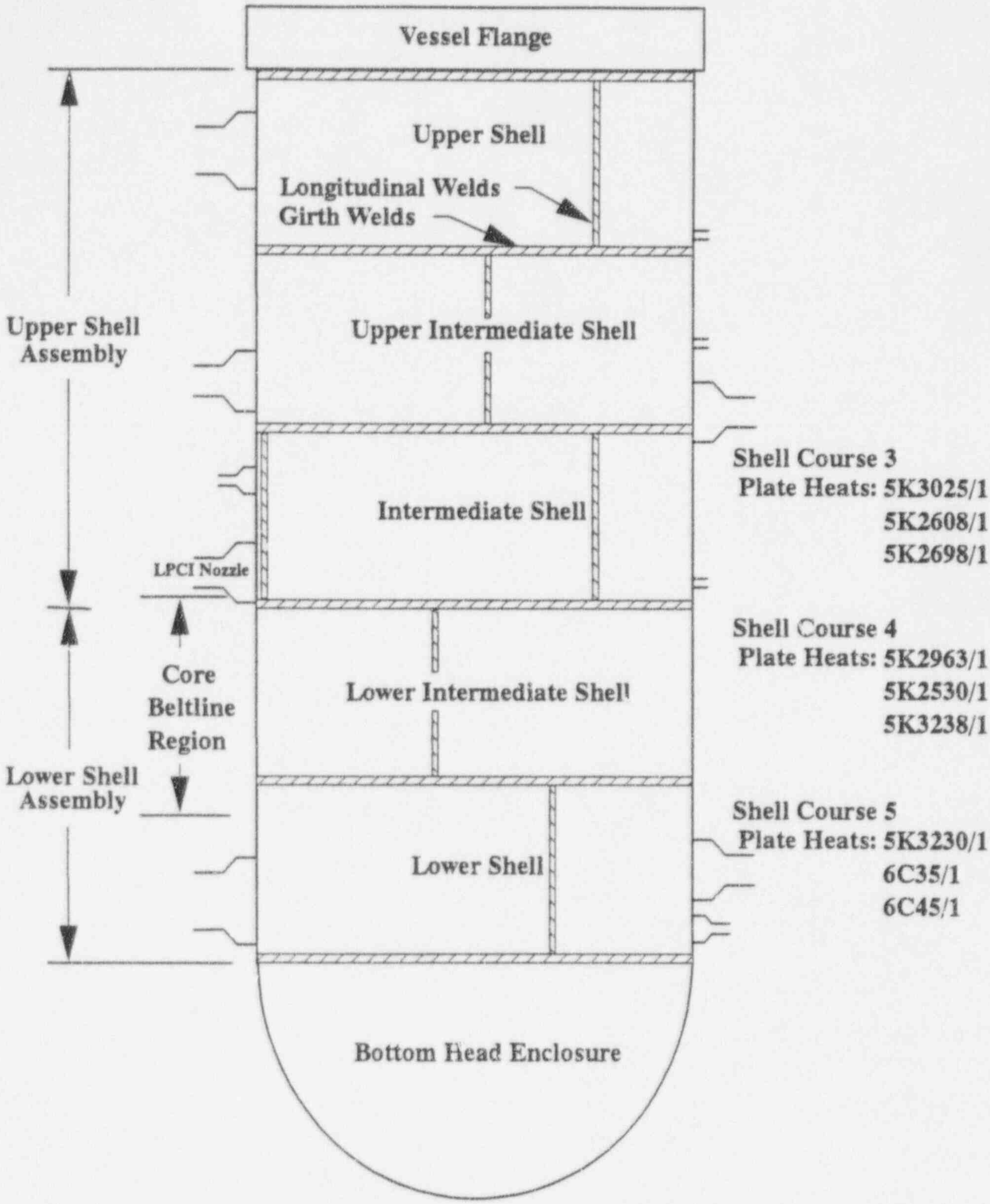

Figure 3-2. Schematic of RPV Showing Identification of Vessel Beltline Plates and Welds

4. PEAK RPV FLUENCE EVALUATION

Flux wires removed from the 30° capsule were analyzed, as described in Section 4.1, to determine flux and fluence received by the surveillance capsule. The lead factor, determined as described in Section 4.2, was used to establish the peak vessel fluence from the flux wire results. Section 4.3 includes 32 EFPY peak fluence estimates at the surface of the vessel and at the 1/4 T location.

4.1 FLUX WIRE ANALYSIS

4.1.1 Procedure

The surveillance capsule contained 9 flux wires: 3 iron, 3 copper, and 3 nickel. Each wire was removed from the capsule, cleaned with dilute acid, weighed, mounted on a counting card, and analyzed for its radioactivity content by gamma spectrometry. Each iron wire was analyzed for Mn-54 content, each nickel wire for Co-58 and each copper wire for Co-60 at a calibrated 4-cm or 10-cm source-to-detector distance with 100-cc Ge(Li) and 170-cc Ge detector systems.

To properly predict the flux and fluence at the surveillance capsule from the activity of the flux wires, the periods of full and partial power irradiation and the zero power decay periods were considered. Operating days for each fuel cycle and the reactor average power fraction are shown in Table 4-1.

From the flux wire activity measurements and power history, reaction rates for Fe-54 (n,p) Mn-54, Cu-63 (n,α) Co-60 and Ni-58 (n,p) Co-58 were calculated. The E>1 MeV fast flux reaction cross sections were determined from past testing at Browns Ferry 3 [10], also a 251 inch, 764 bundle plant, using multiple dosimeter and spectrum unfolding techniques. The cross sections for the iron, copper, and nickel wires are 0.213 barn, 0.00374 barn and 0.274 barn, respectively. These values are consistent with other measured cross section functions determined at VNC from more than 65 spectral determinations for BWRs and for the General Electric Test Reactor using activation monitors and spectral unfolding techniques. These data functions are applied to BWR pressure vessel locations based on water gap (fuel to vessel wall) distances. The cross sections for E>0.1 MeV flux were determined from the measured 1-to-0.1 MeV cross section ratio of 1.6.

4.1.2 Results

The measured activity, reaction rate and full-power flux results for the 30° surveillance capsule are given in Table 4-2. The E>1 MeV flux values were calculated by dividing the wire reaction rate measurements by the corresponding cross sections, factoring in the local power history for each fuel cycle. The fluence result, 1.42×10^{17} n/cm^2 (E>1 MeV) was obtained by multiplying the full-power flux value for the average of iron and copper by the operating time and full power fraction, shown in Table 4-1.

The accuracies of the values in Tables 4-2 for a 2σ deviation are estimated to be:

$\pm$ 5% for dps/g (disintegrations per second per gram)
$\pm$ 10% for dps/nucleus (saturated)
$\pm$ 20% for flux and fluence E>1 MeV
$\pm$ 20% for flux and fluence E>0.1 MeV

4.2 DETERMINATION OF LEAD FACTOR

The flux wires detect flux at a single location. The wires will therefore reflect the power fluctuations associated with the operation of the plant. However, the flux wires are not necessarily at the location of peak vessel flux. A lead factor is required to relate the flux at the wires' location to the peak flux. The lead factor is the ratio of the flux at the surveillance capsule to the flux at the peak inside surface location. The lead factor is a function of the core and vessel geometry and of the distribution of bundles in the core. The lead factor was generated for the vessel geometry, using a typical fuel cycle to determine power shape and void distribution. The methods used to calculate the lead factor are discussed below.

4.2.1 Procedure

Determination of the lead factor for the RPV inside wall was made using a combination of two separate two-dimensional finite difference computer analyses. The first of these established the relative azimuthal variation of fluence at the vessel surface and 1/4 T depth. The second analysis determined the relative variation of flux with elevation. The azimuthal and axial distribution results were combined to provide the ratio of flux, or the lead factor, between the surveillance capsule location and the peak flux locations.

The DORT computer program, which utilizes the discrete ordinates method to solve the Boltzmann transport equation in two dimensions, was used to calculate the spatial flux distribution produced by a fixed source of neutrons in the core region. The azimuthal distribution was obtained with a model specified in (R,θ) geometry, assuming eighth-core symmetry with reflective boundary conditions at 0° and 45°. Calculations were performed using neutron cross-sections from a 26 energy group set, with angular dependence of the scattering cross-sections approximated by a third-order Legendre polynomial expansion.

A schematic of the (R,θ) vessel model is shown in Figure 4-1. A total of 131 radial intervals and 90 azimuthal intervals were used. The model consists of an inner and outer core region, the shroud, water regions inside and outside the shroud, and the vessel wall. The core region material compositions and neutron source densities were representative of conditions at an elevation 75 inches above the bottom of active fuel, which is near the elevation of the wires. Flux as a function of azimuth and radius was calculated, establishing the azimuth of the peak flux and its magnitude relative to the flux at the wires' location of 30°.

The calculation of the axial flux distribution was performed in (R,Z) geometry, using a simplified cylindrical representation of the core configuration and realistic simulations of the axial variations of power density and coolant mass density. The core description was based on conditions near the azimuth angle of 25° where the edge of the core is closest to the vessel wall. The elevation of the peak flux was determined, as well as its magnitude relative to the flux at the surveillance capsule elevation.

4.2.2 Results

The two-dimensional computations indicate the flux to be a maximum 25.25° past the RPV quadrant references (0°, 90°, etc.), at an elevation about 82 inches above the bottom of active fuel. The peak closest to the 30° location of the surveillance capsule removed is at 25.25°, as shown in Figure 4-2. The relative flux distribution versus elevation is shown in Figure 4-3. The distribution calculations establish the lead factor between the surveillance capsule location and the peak location at the inner vessel wall. The calculated flux at the capsule (R,θ) position along the midplane was modified by an appropriate ratio derived from the (R,Z) model to account for the actual capsule elevation position. The resulting computed surveillance capsule flux is 9.4×10^8 n/cm^2-s. The peak flux at vessel surface from the transport calculation, incorporating modification due to differences between (R,θ) and (R,Z) models, is 9.3×10^8 n/cm^2-s. Therefore the lead factor is 9.4/9.3=1.01.

The transport calculation of surveillance capsule flux, 9.4×10^8 n/cm²-s, is about 25% higher than the measured (flux wire analysis) surveillance capsule result of 7.5×10^8 n/cm²-s. This may be due to the conservative methods of the transport computation and to uncertainties in physical dimensions, such as using nominal rather than actual vessel radius. The uncertainty associated with vessel radius has little, if any, effect on the lead factor, since for the lead factor the fluence values at two locations with the same radius are being ratioed. The lead factor computed here was based on fuel cycles 1 through 5 whereas that determined in [11] was based on fuel cycle 1 only.

The fracture toughness analysis is based on a 1/4 T depth flaw in the beltline region, so the attenuation of the flux to that depth is considered. This attenuation is calculated according to Reg. Guide 1.99 requirements, as shown in the next section.

4.3 ESTIMATE OF 32 EFPY FLUENCE

The inside surface fluence (f_{surf}) at 32 EFPY is determined from the flux wire fluence for 6.01 EFPY of 1.42×10^{17} n/cm², using the lead factor of 1.01. The time period 32 EFPY is based on 40-year operation at an 80% capacity factor. The resulting 32 EFPY fluence value at the peak vessel inside surface is:

$$f_{surf} = 1.42\times10^{17} * (32/6.01)/1.01$$

$$f_{surf} = 7.5\times10^{17}\ \text{n/cm}^2$$

This fluence represents the peak value, which occurs in the lower-intermediate shell (No.4) and will be conservatively applied to lower shell (No.5). The peak surface fluence is about 14% greater than the nominal value (6.6×10^{17} n/cm²) calculated from the first cycle dosimetry [11]; however, within the 20% accuracy expected as reported in Section 4.1.2. The bottom of the intermediate shell (No.3) is 143.2 inches from the bottom of active fuel. The fluence at this elevation can be conservatively calculated using information in Figure 4-3 as:

$$f_{surf} = 7.5\times10^{17} * (0.66) = 4.94\times10^{17}\ \text{n/cm}^2 \qquad \text{for the intermediate shell}$$

The fluence at the LPCI nozzle in the intermediate shell (No. 3) has an additional relative decrease in fluence due to the azimuthal variation shown in Figure 4-2. Since a LPCI nozzle is at a relative

angular position of 35°, the fluence at the LPCI nozzle is calculated as follows:

$f_{surf} = 7.5x10^{17}*(0.66)*(0.82) = 4.05x10^{17}$ n/cm^2 for the LPCI nozzle

The 1/4 T fluence (f) is calculated as follows, according to the Reg. Guide 1.99 [7]:

$$f = f_{surf}*(e^{-0.24x}) \tag{4-1},$$

where x = distance, in inches, to the 1/4 T depth. The vessel beltline lower-intermediate shell and intermediate shell are 6.10 inches thick. The corresponding depth x is 1.53 inches. Equation 4-1 yields:

$f = f_{surf}(0.69) = 5.2x10^{17}$ n/cm^2 for the lower-intermediate shell

$f = f_{surf}(0.69) = 3.42x10^{17}$ n/cm^2 for the intermediate shell

$f = f_{surf}(0.69) = 2.81x10^{17}$ n/cm^2 for the LPCI nozzle

The impact of these revised fluences on the P-T curves is discussed in Section 7.

Table 4-1

SUMMARY OF CONDENSED POWER HISTORY

Cycle	Cycle Dates	Operating Days	Full Power Fraction
1	10/12/86 - 02/13/88	453	0.825
2	04/16/88 - 09/15/89	518	0.892
3	11/20/89 - 12/16/90	392	0.930
4	02/22/91 - 09/12/92	564	0.943
5	11/12/92 - 03/05/94	473	0.977
		2400 (total)	0.914 (average)

Table 4-2

SURVEILLANCE CAPSULE FLUX AND FLUENCE FOR IRRADIATION FROM START-UP TO 3/5/94

Wire (Element)	dps/g Element (at end of Irradiation)	Reaction Rate [dps/nucleus (saturated)]	Full Power Flux [a] (n/cm^2-s) >1 MeV	Full Power Flux [b] (n/cm^2-s) >0.1 MeV	Fluence (n/cm^2) >1 MeV	Fluence [b] (n/cm^2) >0.1 MeV
Copper G9	9.472 E3	2.801 E-18	7.489 E8	11.982 E8	1.42 E17	2.27 E17
Copper G11	9.306 E3	2.752 E-18	7.358 E8	11.773 E8	1.39 E17	2.22 E17
Copper G12	9.152 E3	2.706 E-18	7.235 E8	11.576 E8	1.37 E17	2.19 E17
Iron G9	8.920 E4	1.595 E-16	7.488 E8	11.981 E8	1.42 E17	2.27 E17
Iron G11	9.079 E4	1.624 E-16	7.624 E8	12.198 E8	1.45 E17	2.32 E17
Iron G12	9.017 E4	1.613 E-16	7.573 E8	12.117 E8	1.44 E17	2.30 E17
Nickel G9	1.306 E6	1.942 E-16	7.088 E8	11.341 E8	1.34 E17	2.14 E17
Nickel G11	1.342 E6	1.996 E-16	7.285 E8	11.656 E8	1.38 E17	2.21 E17
Nickel G12	1.306 E6	1.942 E-16	7.088 E8	11.341 E8	1.34 E17	2.14 E17
				Average [c] =	1.42 E17 $\pm$0.06 E17	2.27 E17 $\pm$0.10E17

[a] Full power flux, based on thermal power of 3293 MW_t
[b] 1.6 times the E >1 MeV results
[c] Nickel is not included in final average

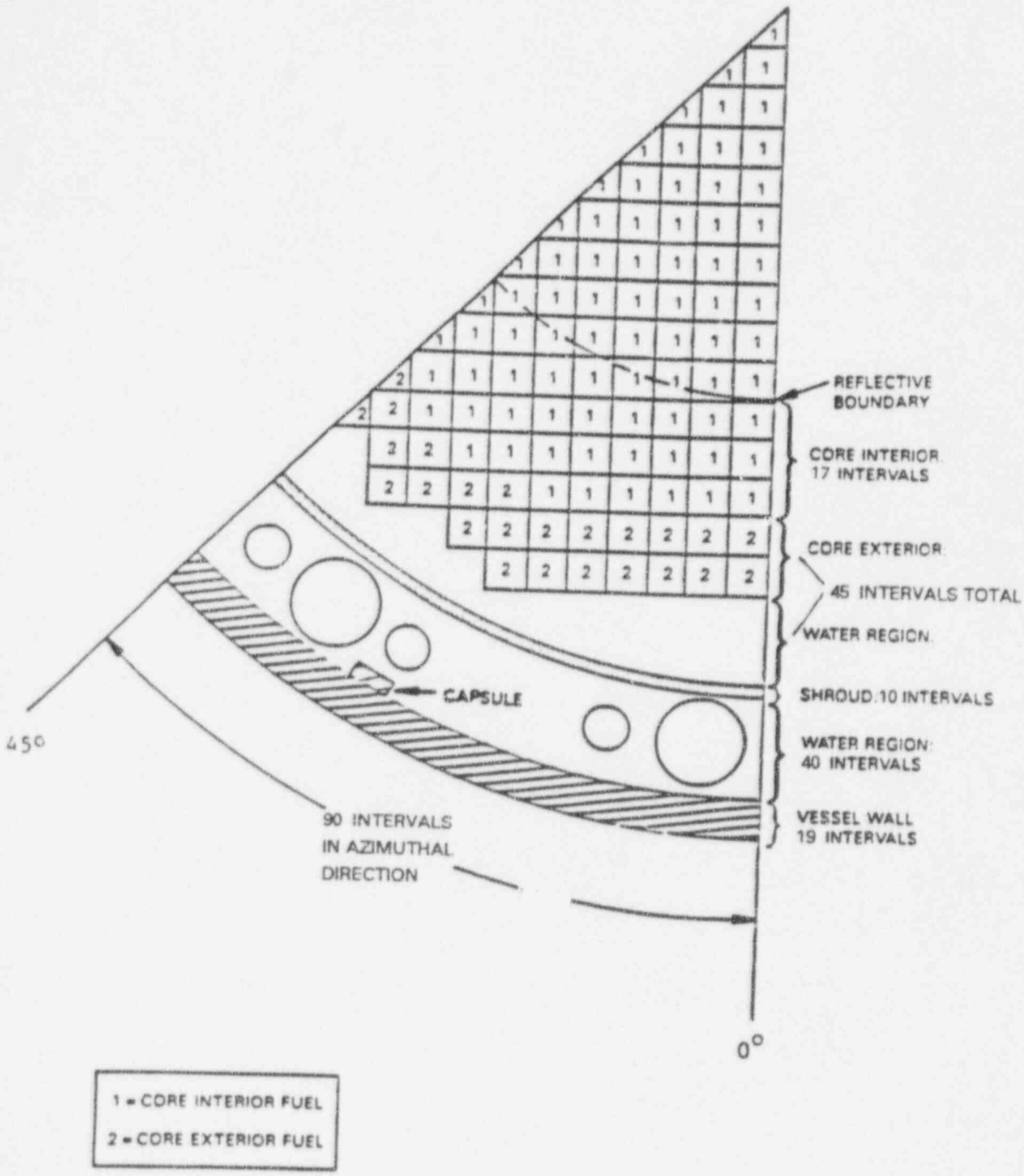

Figure 4-1. Schematic of Model for Azimuthal Flux Distribution Analysis

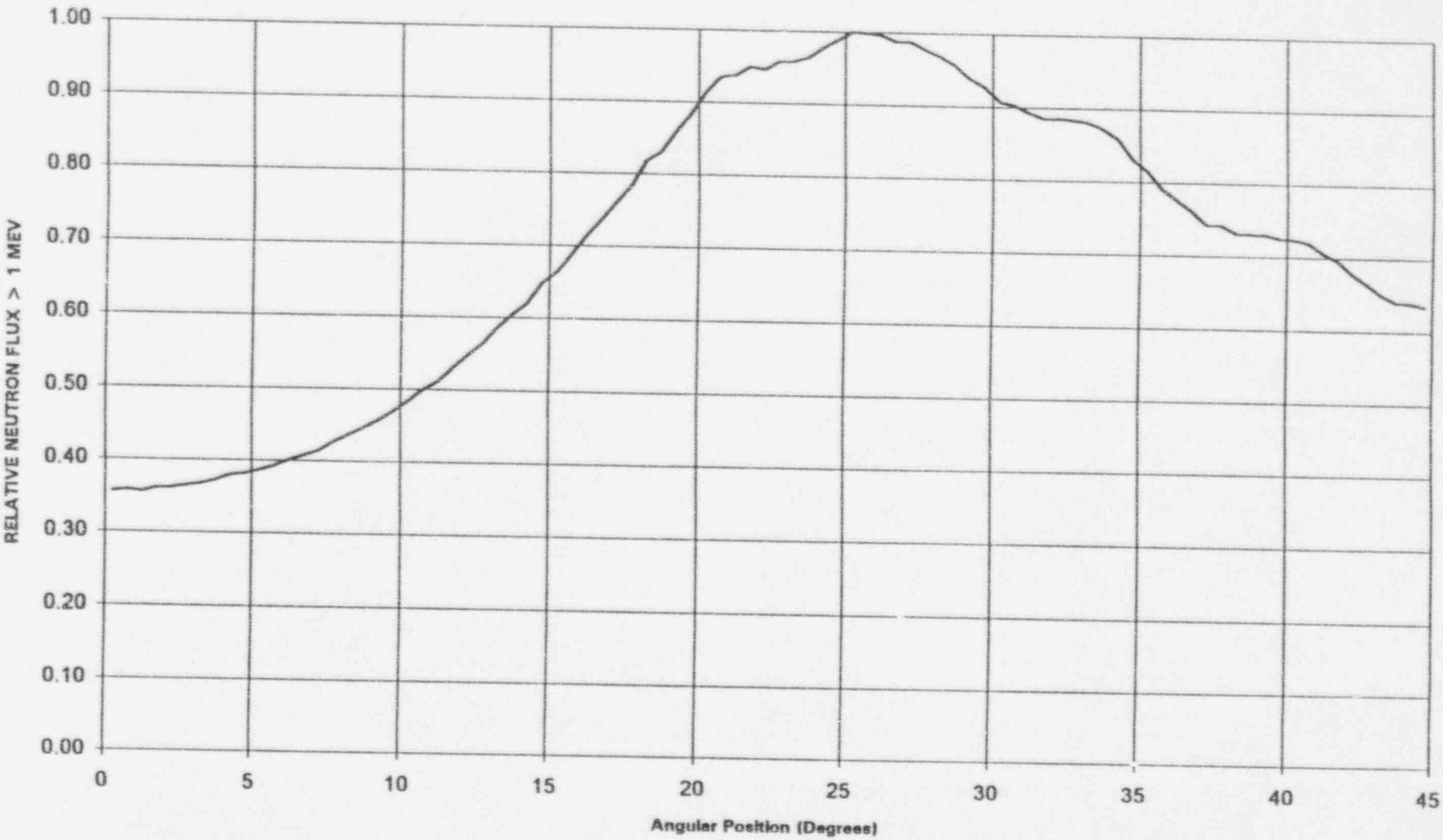

Figure 4-2. Relative Vessel Flux Variation with Angular Position

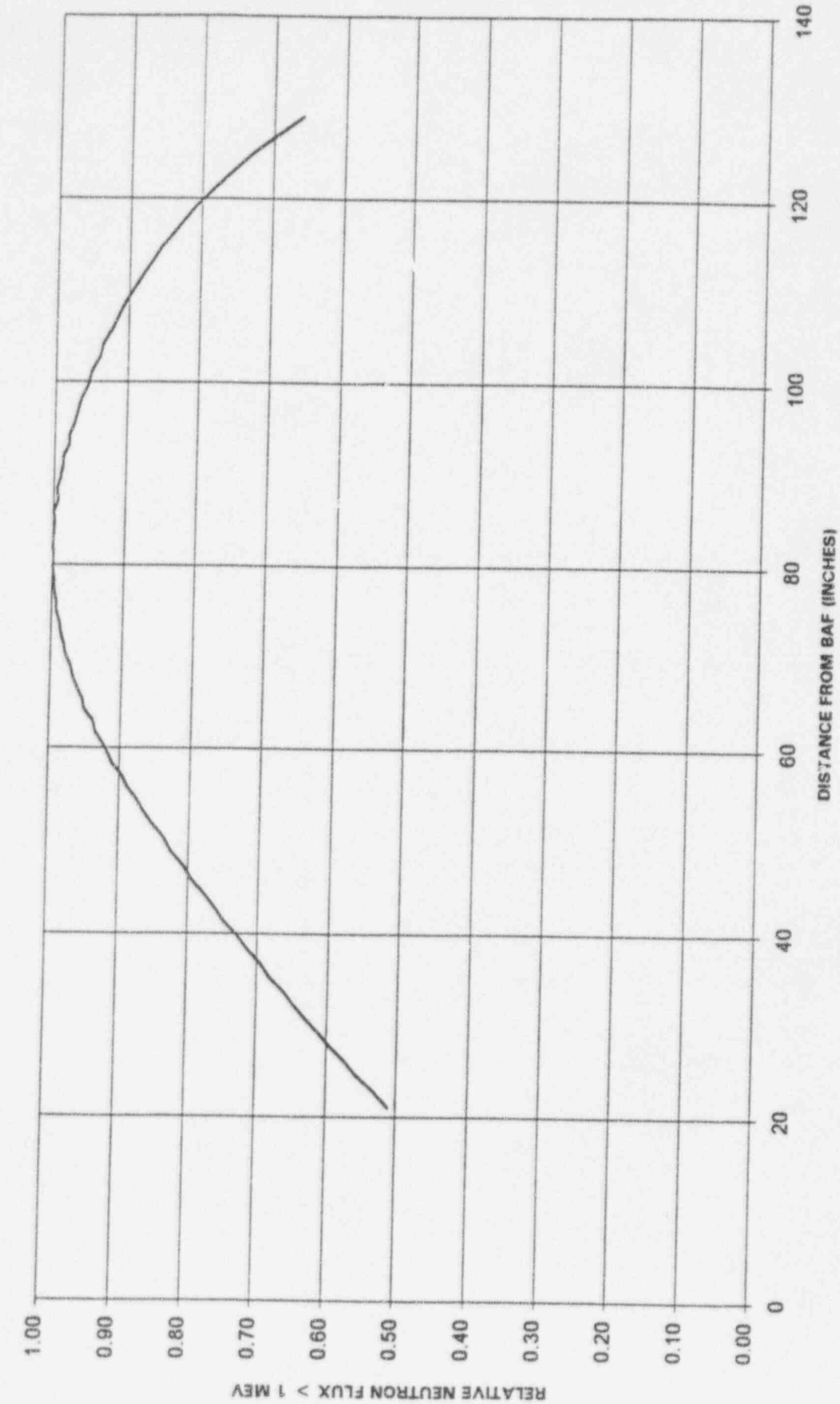

Figure 4-3. Relative Vessel Flux Variation with Elevation

5. CHARPY V-NOTCH IMPACT TESTING

The 36 Charpy specimens recovered from the surveillance capsule were impact tested at temperatures selected to establish the toughness transition and upper shelf of the irradiated RPV materials. In addition, longitudinal unirradiated base, weld, and longitudinal HAZ metal specimens recovered from the Hope Creek site were tested for baseline data. Testing was conducted in accordance with ASTM E23-88 [12].

5.1 IMPACT TEST PROCEDURE

The Vallecitos testing machine used for unirradiated and irradiated specimens was a Riehle Model P1-2 impact machine, serial number R-89916. The maximum energy capacity of the machine is 240 ft-lb, and the test velocity at impact is 15.44 ft/sec.

The test apparatus and operator were qualified using NIST standard reference material specimens. The standards consist of sets of high and low energy specimens, each designed to fail at a specified energy at the standard test temperature of -40°F. According to ASTM E23-88 [12], the test apparatus averaged results must reproduce the NIST standard values within an accuracy of $\pm$5% or $\pm$1.0 ft-lb, whichever is greater. The qualification of the Riehle machine and operator is summarized in Table 5-1.

Charpy V-Notch tests were conducted at temperatures between -100°F and 300°F. The cooling fluid used for both irradiated and unirradiated specimens tested at temperatures below 70°F was ethyl alcohol. At temperatures between 70°F and 200°F, water was used as the temperature conditioning fluid. The specimens were heated in silicon oil above 200°F. Cooling of the conditioning fluids was done by heat exchange with liquid nitrogen; heating was done by an immersion heater. The liquid bath was mechanically stirred to maintain uniform temperatures. The bath temperature was measured with a calibrated thermocouple. After equilibrium at the test temperature for at least 5 minutes, the specimens were manually transferred with centering tongs to the Charpy test machine and impacted in less than 5 seconds.

For each Charpy V-Notch specimen the test temperature, energy absorbed, lateral expansion, and percent shear were evaluated. In addition, for the irradiated specimens, photographs were taken of fracture surfaces. Lateral expansion was measured according to specified methods [12]. Percent shear was determined using method number 1 of Subsection 11.2.4.3 of ASTM E23-88 [12], which involved measuring the length and width of the cleavage surface in inches and determining the percent shear value from Table 2 of ASTM E23-88 [12].

5.2 IMPACT TEST RESULTS

Thirty-five unirradiated Charpy V-Notch specimens of 12 base, 11 weld, and 12 HAZ materials were tested at temperatures (-100°F to 300°F) selected to define the toughness transition and upper shelf portion of the fracture toughness curves. The absorbed energy, lateral expansion, and percent shear data are listed in Table 5-2. Plots of absorbed energy data for unirradiated base, weld, and HAZ metals are presented in Figures 5-1, 5-6, and 5-11, respectively. Lateral expansion plots for base and weld metals are presented in Figures 5-4 and 5-9, respectively.

Twelve Charpy V-Notch specimens each of irradiated base, weld, and HAZ material were tested at temperatures (-100°F to 300°F) selected to define the toughness transition and upper shelf portions of the fracture toughness curves. One HAZ specimen (specimen 619) partially broke by ductile tearing at 233 ft-lb (see Appendix A). The absorbed energy, lateral expansion, and percent shear data are listed for each material in Table 5-3. Plots of absorbed energy data for irradiated base, weld and HAZ materials are presented in Figures 5-2, 5-7, and 5-12, respectively. Lateral expansion plots for base and weld materials are presented in Figures 5-5 and 5-10, respectively. The irradiated impact energy curves are plotted along with their corresponding unirradiated curve in Figures 5-3 and 5-8 for base and weld specimens, respectively. The fracture surface photographs and a summary of the test results for each specimen are contained in Appendix A.

The plate and weld data sets are fit with the hyperbolic tangent function developed by Oldfield for the EPRI Irradiated Steel Handbook [13]:

$$Y = A + B * \mathrm{TANH}\,[(T - T_0)/C],$$

where Y = impact energy or lateral expansion, T = test temperature, and A, B, T_0 and C are determined by non-linear regression.

The TANH function is one of the few continuous functions with a shape characteristic of low alloy steel fracture toughness transition curves. The curve fits were generated by fixing the lower shelf to 2.2 ft-lb for Charpy energy and 1.0 mil for lateral expansion and setting the upper shelf free.

5.3 IRRADIATED VERSUS UNIRRADIATED CHARPY V-NOTCH PROPERTIES

The irradiated and unirradiated Charpy V-Notch data curves were used to estimate the values given in Table 5-4: 30 ft-lb, 50 ft-lb and 35 MLE index temperatures. Transition temperature shift values are determined as the change in the temperature at which 30 ft-lb impact energy is achieved, as required in ASTM E185-82 [6]. The resulting shifts in Charpy curves are discussed in the next section. The USE values are determined by averaging the Charpy data at 100% shear.

5.4 COMPARISON TO PREDICTED IRRADIATION EFFECTS

5.4.1 Irradiation Shift

The measured transition temperature shifts for the plate and weld materials were compared to the predictions calculated according to Regulatory Guide 1.99, Revision 2 [7]. The inputs and calculated values for irradiated shift are as follows:

Plate:
- Copper = 0.09%
- Nickel = 0.64%
- CF = 58
- fluence = 1.42×10^{17} n/cm^2
- Reg. Guide 1.99 ΔRT_{NDT} = 8°F
- Reg. Guide 1.99 $\Delta RT_{NDT} \pm 2\sigma_\Delta$(34°F) = -26°F min, 42°F max.
- Measured 30 ft-lb shift = 4 °F

Weld:
- Copper = 0.08%
- Nickel = 0.59%
- CF = 105
- fluence = 1.42×10^{17} n/cm^2
- Reg. Guide 1.99 ΔRT_{NDT} = 15°F
- Reg. Guide 1.99 $\Delta RT_{NDT} \pm 2\sigma_\Delta$(56°F) = -41°F min, 71°F max.
- Measured 30 ft-lb shift = 61°F

The weight percents of Cu and Ni are the average of the plate and weld results in Table 3-3. CF shown above is the chemistry factors from Tables 1 or 2 of Reg. Guide 1.99 [7]. The fluence factor from Figure 1 of [7] is 0.14. The measured shifts of 4°F for the plate and 61°F for the weld are below and above the predicted shifts of 8°F and 15°F, respectively and are within the bounds of the Reg. Guide 1.99 prediction including uncertainty of 2σ.

5.4.2 <u>Change in USE</u>

Figure 2 of Reg. Guide 1.99 was used with copper and fluence data above to predict decrease in USE of 7% for the plate and decrease in USE of approximately 8% for the weld. The measured decrease in USE is 19 ft-lb (14% decrease) for the plate; this value is greater than the Reg. Guide 1.99 prediction. The weld material shows a measured decrease in USE of 8 ft-lb (5% decrease) which is less than the Reg. Guide 1.99 prediction.

Table 5-1

VALLECITOS QUALIFICATION TEST RESULTS USING NIST STANDARD REFERENCE SPECIMENS

	Specimen Identification	Bath Medium	Test Temperature (°F)	Energy Absorbed (ft-lb)	Acceptable Range (ft-lb)
Vallecitos	HH-40 229	Ethyl Alcohol	-40	75.0	
Riehle Machine	HH-40 384	Ethyl Alcohol	-40	74.5	
(tested 6/28/94)	HH-40 980	Ethyl Alcohol	-40	70.5	
	HH-40 1152	Ethyl Alcohol	-40	72.5	
	HH-40 1172	Ethyl Alcohol	-40	75.0	
			Average	73.5	74.9 ± 3.7 pass
	LL-39 080	Ethyl Alcohol	-40	13.5	
	LL-39 095	Ethyl Alcohol	-40	13.0	
	LL-39 631	Ethyl Alcohol	-40	13.5	
	LL-39 775	Ethyl Alcohol	-40	13.5	
	LL-39 930	Ethyl Alcohol	-40	13.0	
			Average	13.3	13.2 ± 1.0 pass

Table 5-2

UNIRRADIATED CHARPY V-NOTCH IMPACT TEST RESULTS

Specimen Type	Specimen [a] Identification	Test Temperature (°F)	Fracture Energy (ft-lb)	Lateral Expansion (mils)	Percent Shear (Method 1) (%)
Base:	4	-80	10	15	10
Heat 5K3238/1,	3	-40	12.5	15	8
Longitudinal	12	-10	52.5	41	29
	2	0	34.5	36.5	24
	11	20	62.5	49	43
	1	40	30	35	38
	9	50	74.5	57	53
	10	70	99.5	75	67
	5	80	113.5	89	87
	6	120	139.5	94	100
	7	200	139.5	92.5	100
	8	300	141	92	100
Weld:	4	-80	11.5	14	15
Heats D53040	9	-60	27.5	26.5	27
Flux 1125-02205	3	-40	36.5	32	21
	10	-20	78.5	66	45
	2	0	89	63	55
	11	10	58	49	37
	1	40	102	70	74
	5	80	118.5	77	80
	6	120	153	89	100
	7	200	151.5	96.5	100
	8	300	187	84	100
HAZ:	9	-100	16.5	11.5	11
Longitudinal	4	-80	106.5	71.5	54
	3	-40	13.5	14.5	13
	11	-10	136.5	81	74
	2	0	137.5	88	72
	12	20	160	81	100
	1	40	98.5	64	82
	5	80	160.5	83	100
	6	120	104	73	100
	7	200	205	80.5	100
	10	200	169	85	100
	8	300	123	71.5	100

[a] arbitrary numbering of specimen I.D.

Table 5-3

IRRADIATED CHARPY V-NOTCH IMPACT TEST RESULTS

	Specimen Identification	Test Temperature (°F)	Fracture Energy (ft-lb)	Lateral Expansion (mils)	Percent Shear (Method 1) (%)
Base:	614	-80	7	6.5	3
Heat 5K3238/1,	604	-50	8.5	10	6
Longitudinal,	603	-40	32.5	29.9	15
f=1.42x10^{17} n/cm^2	606	-20	7	8.5	18
	612	0	42	37	16
	607	40	55	50.5	52
	610	60	97	77	60
	611	70	105	84.5	79
	609	80	115	78	85
	608	120	113.5	80	100
	613	200	115.5	81	100
	605	300	133	92	100
Weld:	594	-80	5.5	9.5	12
Heats, D53040	597	-40	22.5	20	17
Flux 1125-02205,	595	-10	31	27	26
f=1.42x10^{17} n/cm^2	592	0	19.5	22.5	34
	596	20	59.5	48.5	39
	599	40	88.5	72	50
	601	50	61	44	58
	593	80	112.5	69	77
	598	120	147.5	92	100
	591	150	154.5	90	100
	602	200	144.5	91	100
	600	300	178.5	88	100
HAZ:	616	-100	70	48	33
Longitudinal	624	-80	85	59	44
f=1.42x10^{17} n/cm^2	626	-40	9.5	10	26
	623	-10	59	41	43
	622	0	128.5	79	79
	621	40	41	34	41
	618	70	153	84	100
	617	80	112.5	75	92
	620	120	80.5	59	100
	615	150	172.5	78	100
	625	200	85	68	100
	619	300	>233	61	100

Table 5-4

SIGNIFICANT RESULTS OF IRRADIATED AND UNIRRADIATED CHARPY V-NOTCH DATA

Material	Index Temperature (°F) E=30 ft-lb	Index Temperature (°F) E=50 ft-lb	Index Temperature MLE=35 mil	Upper Shelf [a] Energy (ft-lb)
PLATE: Heat 5K3238/1, Longitudinal				
Unirradiated	-9.16	19.34	-0.73	140 / 91
Irradiated (f=1.42x10^{17} n/cm^2)	-5.31	17.78	2.19	121 / 79
Difference	3.85	-1.56	2.91	19 / 12 (14%)

Reg. Guide 1.99, Rev 2 ΔRtndt [b]: **8** 1.99, Rev 2 % Decrease in USE [c]: **(7%)**
Reg. Guide 1.99, Rev 2 ($\Delta \pm 2\sigma$) [b]: **-26 to 42**

Material	Index Temperature (°F) E=30 ft-lb	Index Temperature (°F) E=50 ft-lb	Index Temperature MLE=35 mil	Upper Shelf [a] Energy (ft-lb)
WELD: Heat/Lot D53040/1125-02205				
Unirradiated	-69.62	-29.70	-44.44	164
Irradiated (f=1.42x10^{17} n/cm^2)	-8.73	18.57	5.00	156
Difference	60.89	48.27	49.44	8 (5%)

Reg. Guide 1.99, Rev 2 ΔRtndt [b]: **15** 1.99, Rev 2 % Decrease in USE [c]: **(8.5%)**
Reg. Guide 1.99, Rev 2 ($\Delta \pm 2\sigma$) [b]: **-41 to 71**

[a] USE values for base are Longitudinal/Transverse orientation; for weld metal are equal. Values determined by averaging the 100% shear Charpy data. Transverse plate USE is taken as 65% of the Longitudinal USE, per USNRC MTEB 5-2 [17].

[b] Determined in Section 5.4.1

[c] See Section 5.4.2

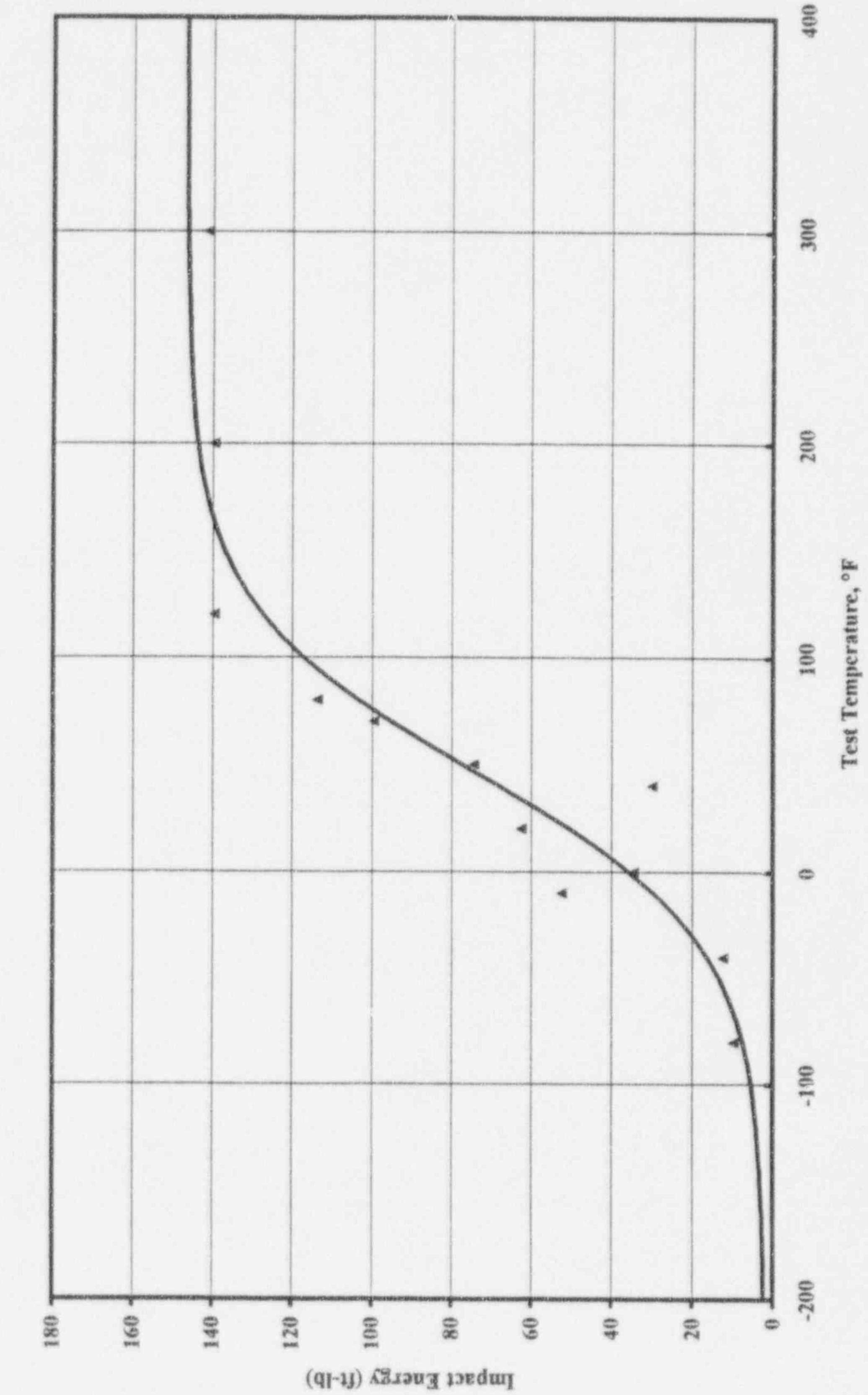

Figure 5-1. Hope Creek 1 Unirradiated
Base Metal Impact Energy

Figure 5-2. Hope Creek 1 Irradiated Base Metal Impact Energy

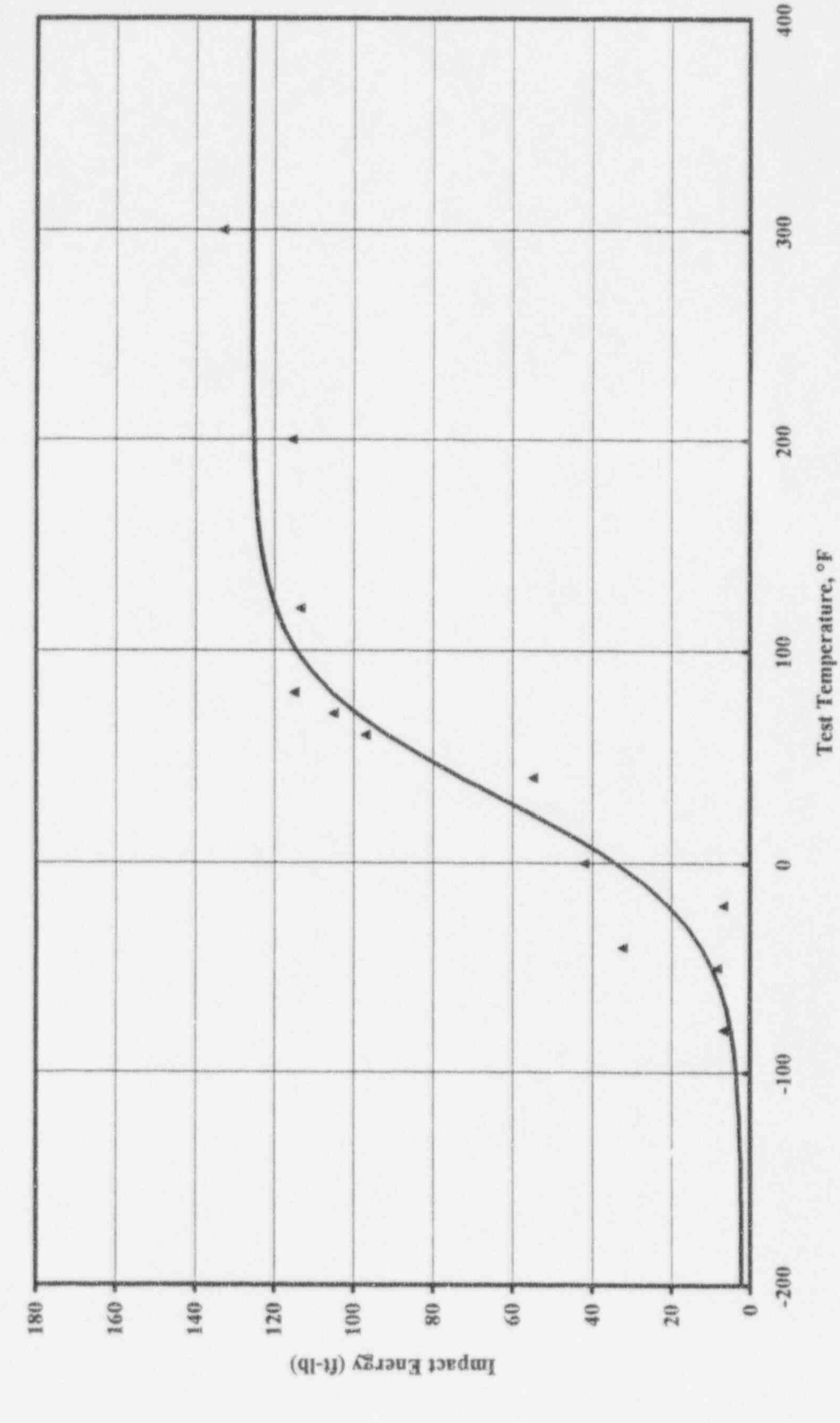

Figure 5-3. Hope Creek 1 Unirradiated and Irradiated Base Metal Impact Energy

14% USE Decrease

4°F RTndt Shift at 30 ft-lb

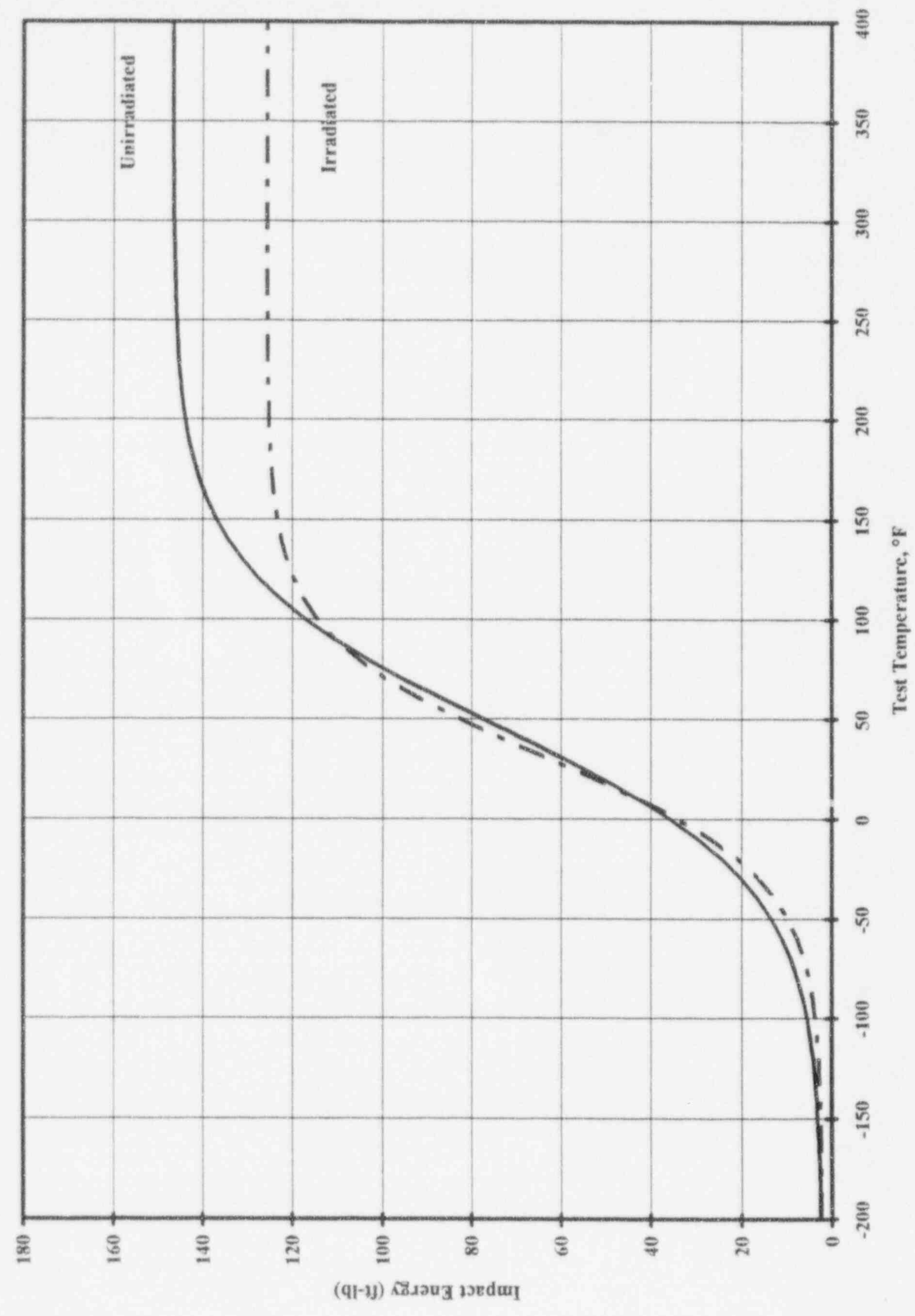

Figure 5-4. Hope Creek 1 Unirradiated
Base Metal Lateral Expansion

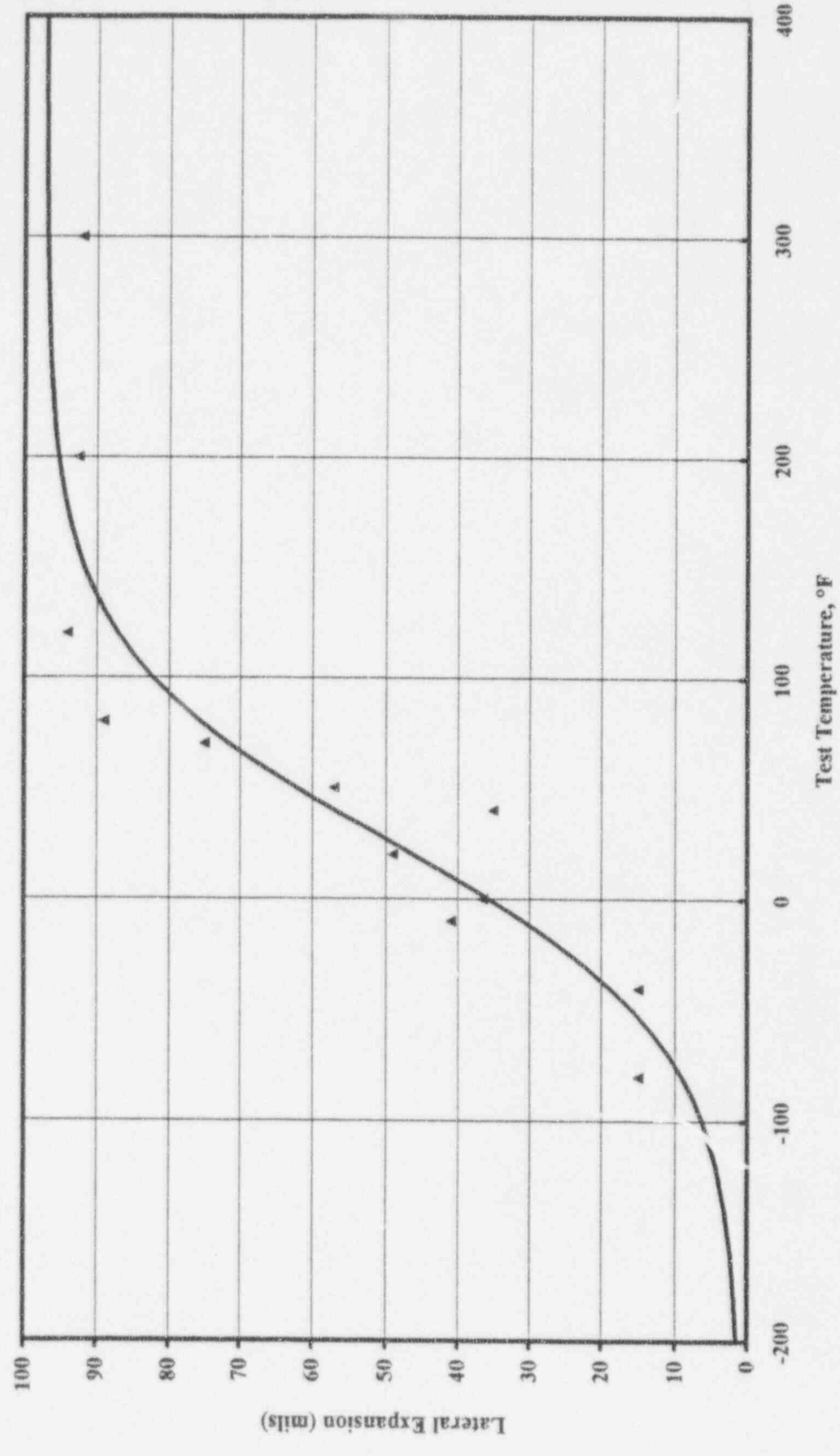

Figure 5-5. Hope Creek 1 Irradiated Base Metal Lateral Expansion

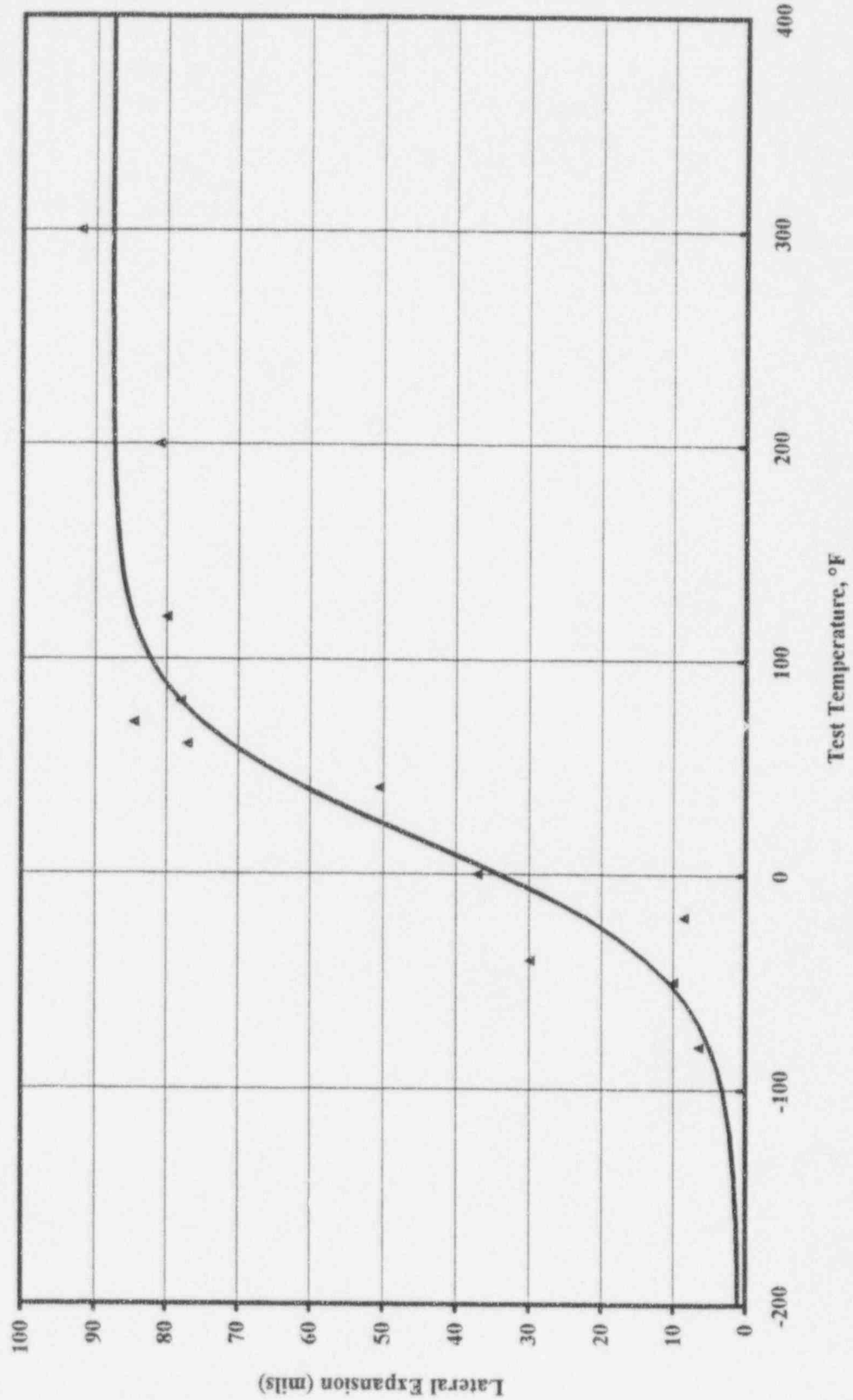

Figure 5-6. Hope Creek 1 Unirradiated
Weld Metal Impact Energy

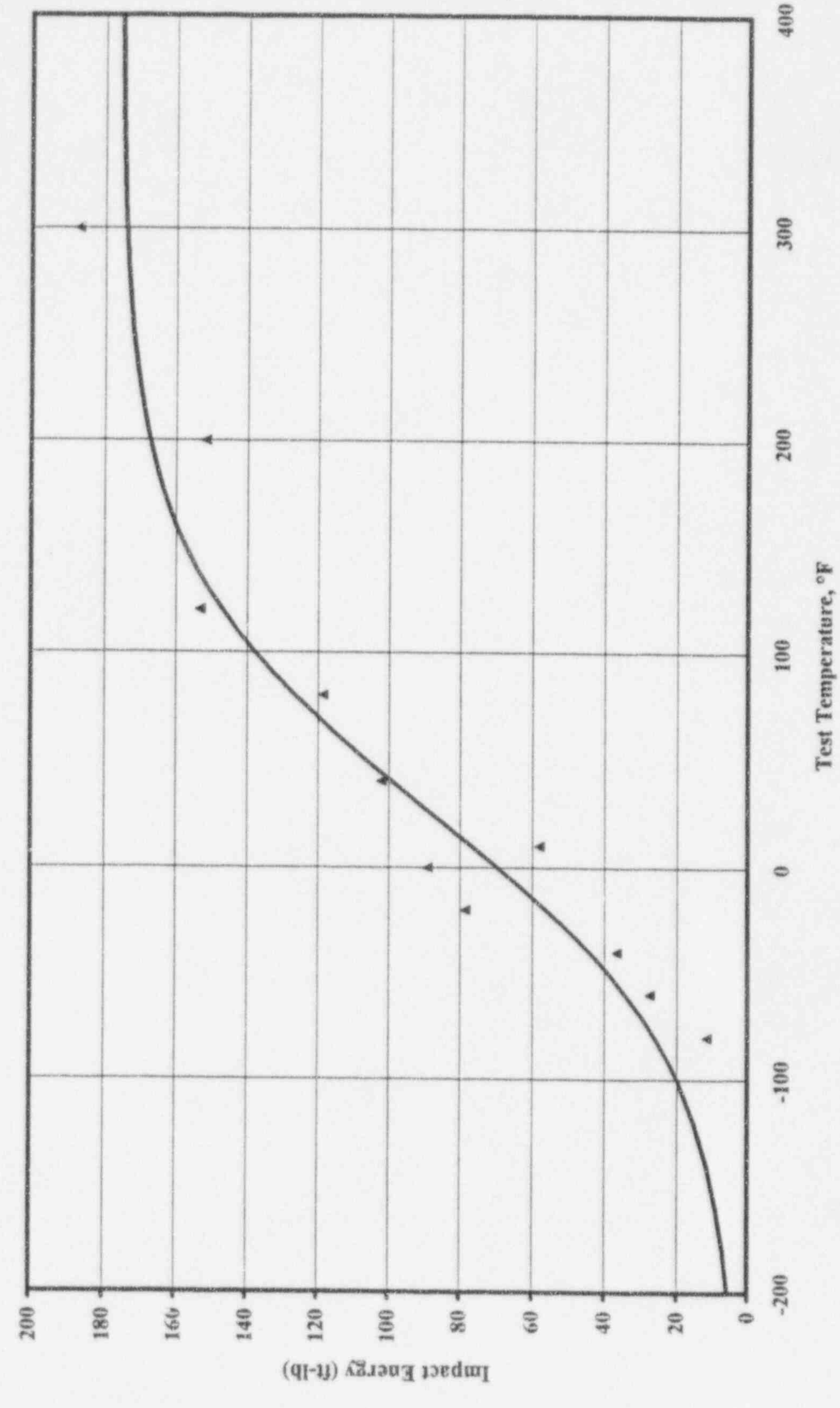

Figure 5-7. Hope Creek 1 Irradiated
Weld Metal Impact Energy

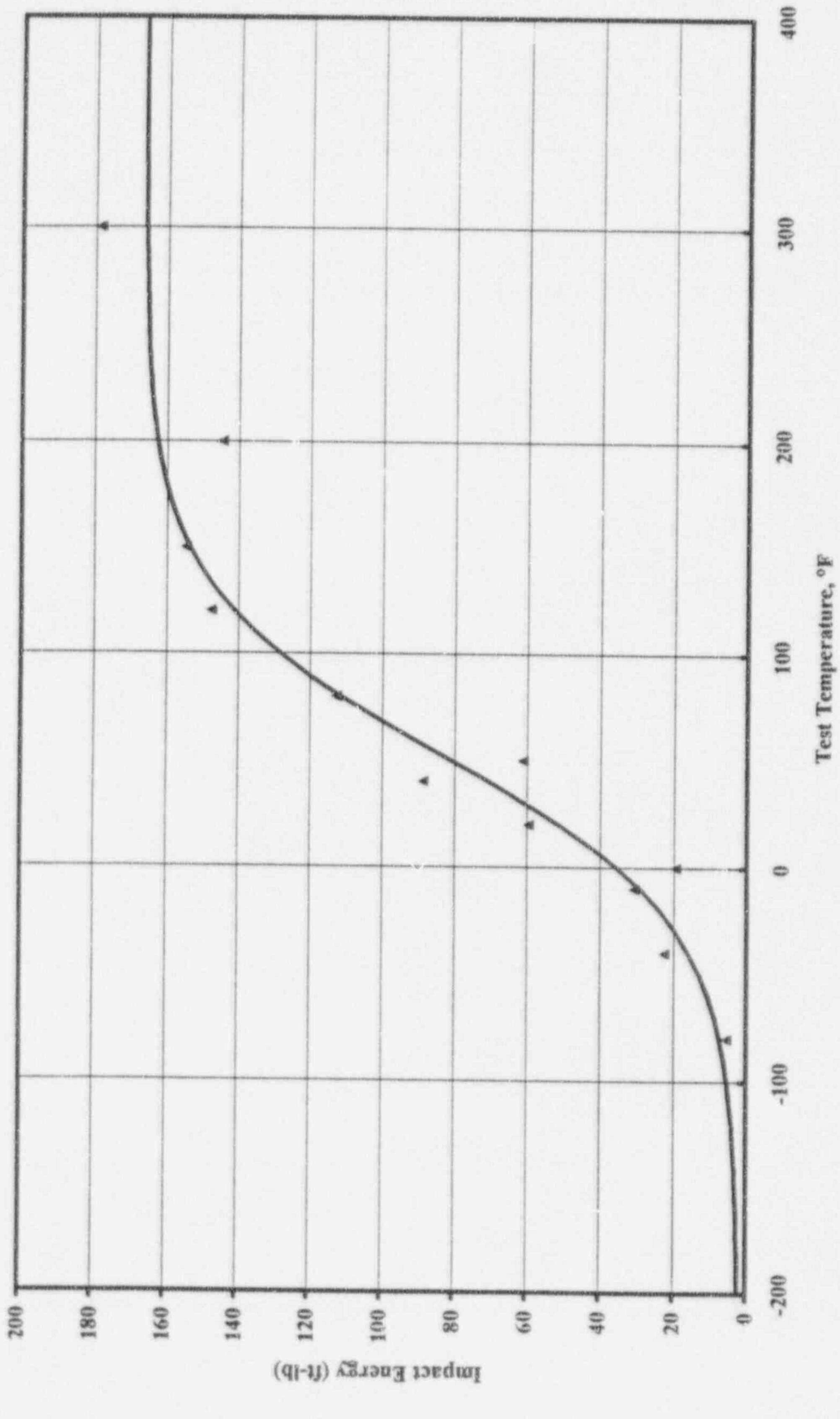

Figure 5-8. Hope Creek 1 Unirradiated and Irradiated Weld Metal Impact Energy

5% USE Decrease

61°F RTndt Shift at 30 ft-lb

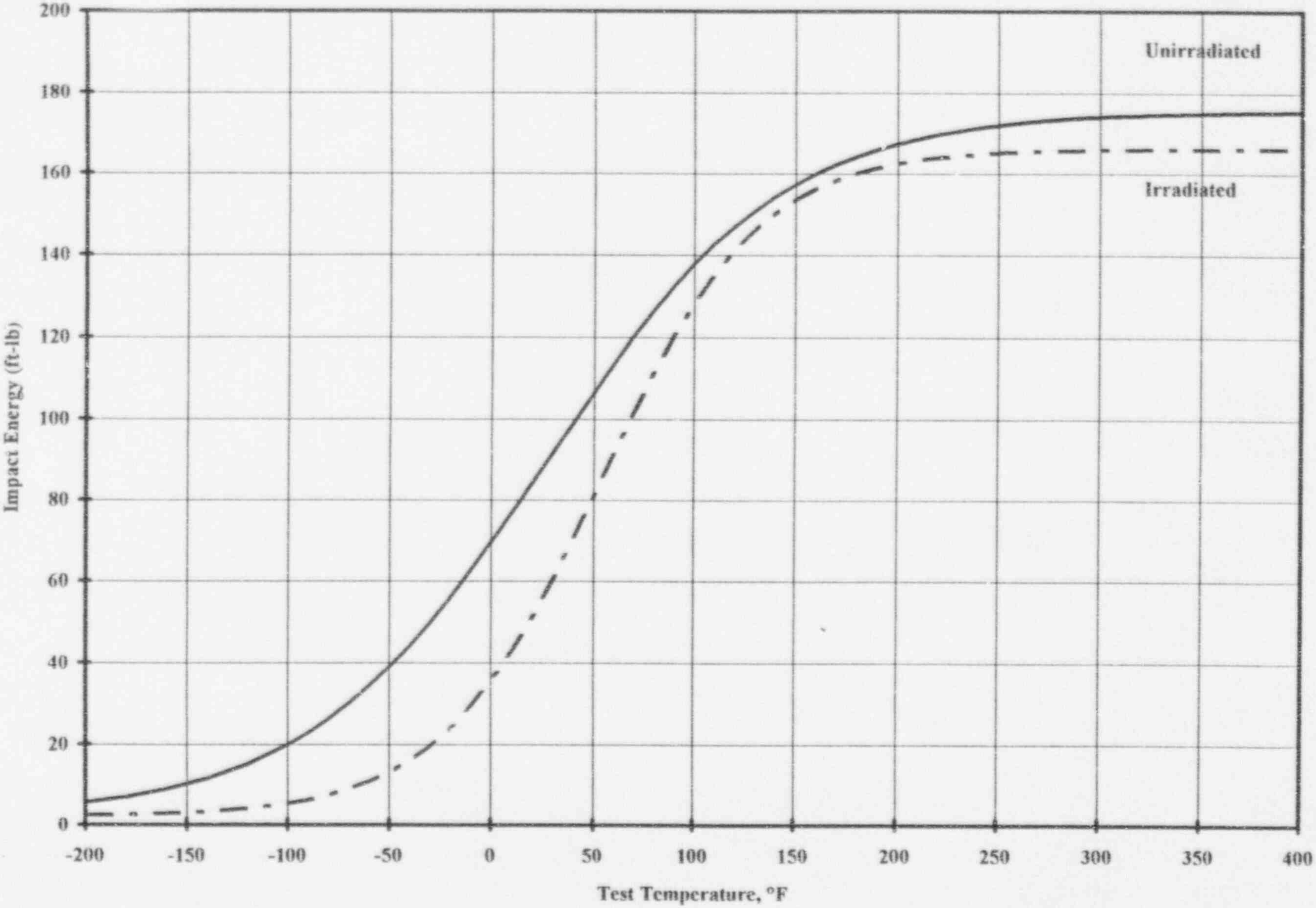

Figure 5-9. Hope Creek 1 Unirradiated Weld Metal Lateral Expansion

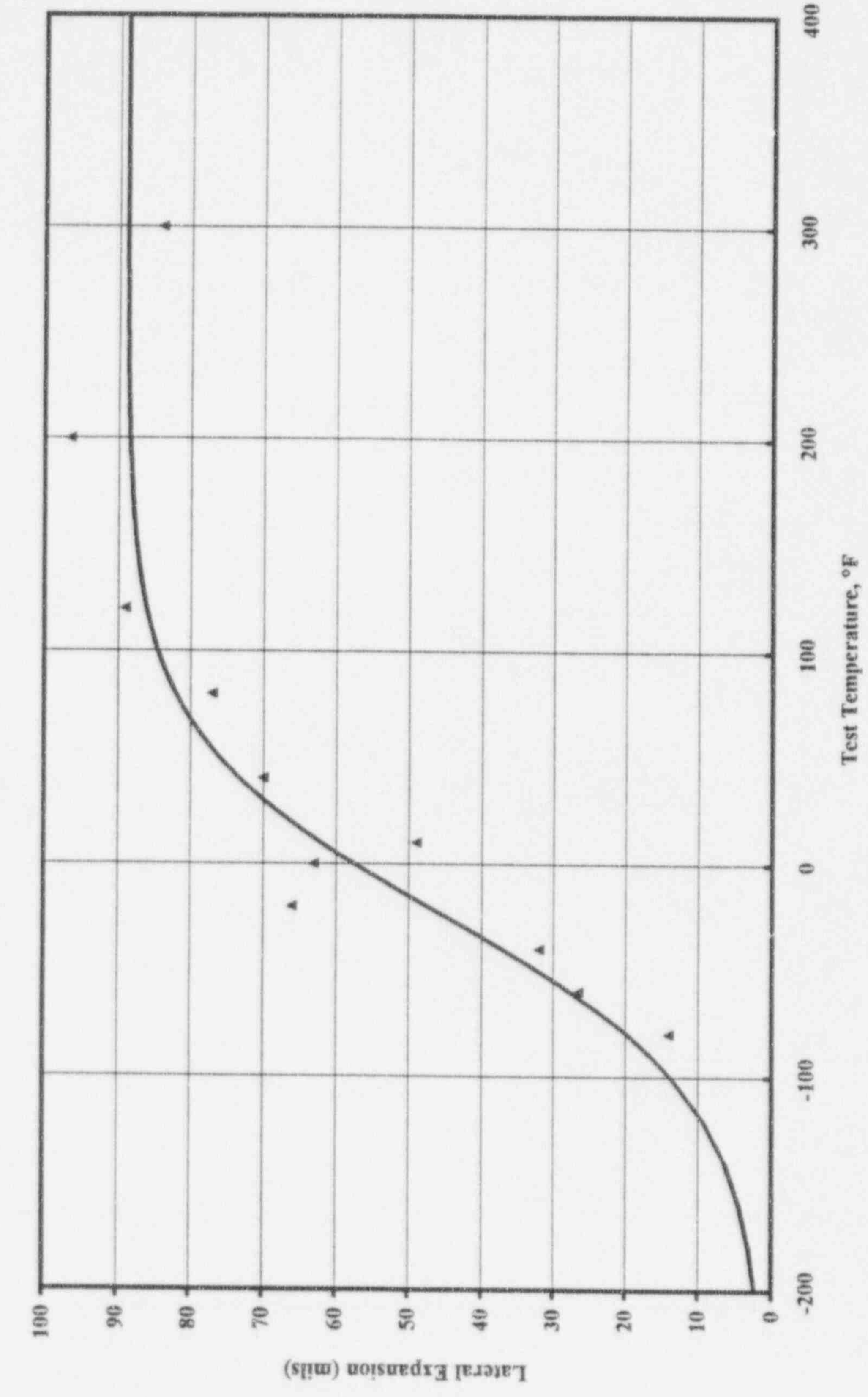

Figure 5-10. Hope Creek 1 Irradiated Weld Metal Lateral Expansion

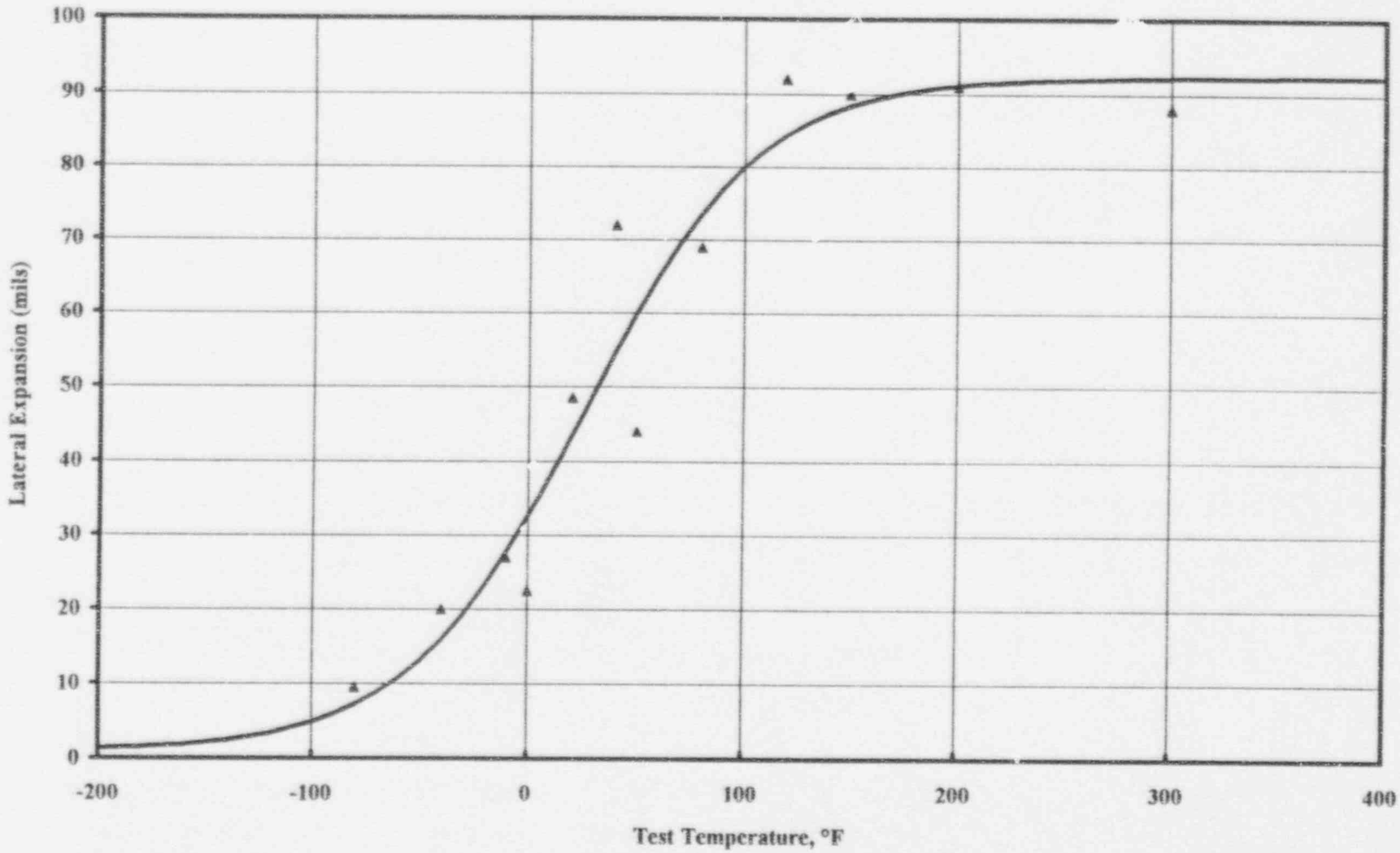

Figure 5-11. Hope Creek 1 Unirradiated
HAZ Metal Impact Energy

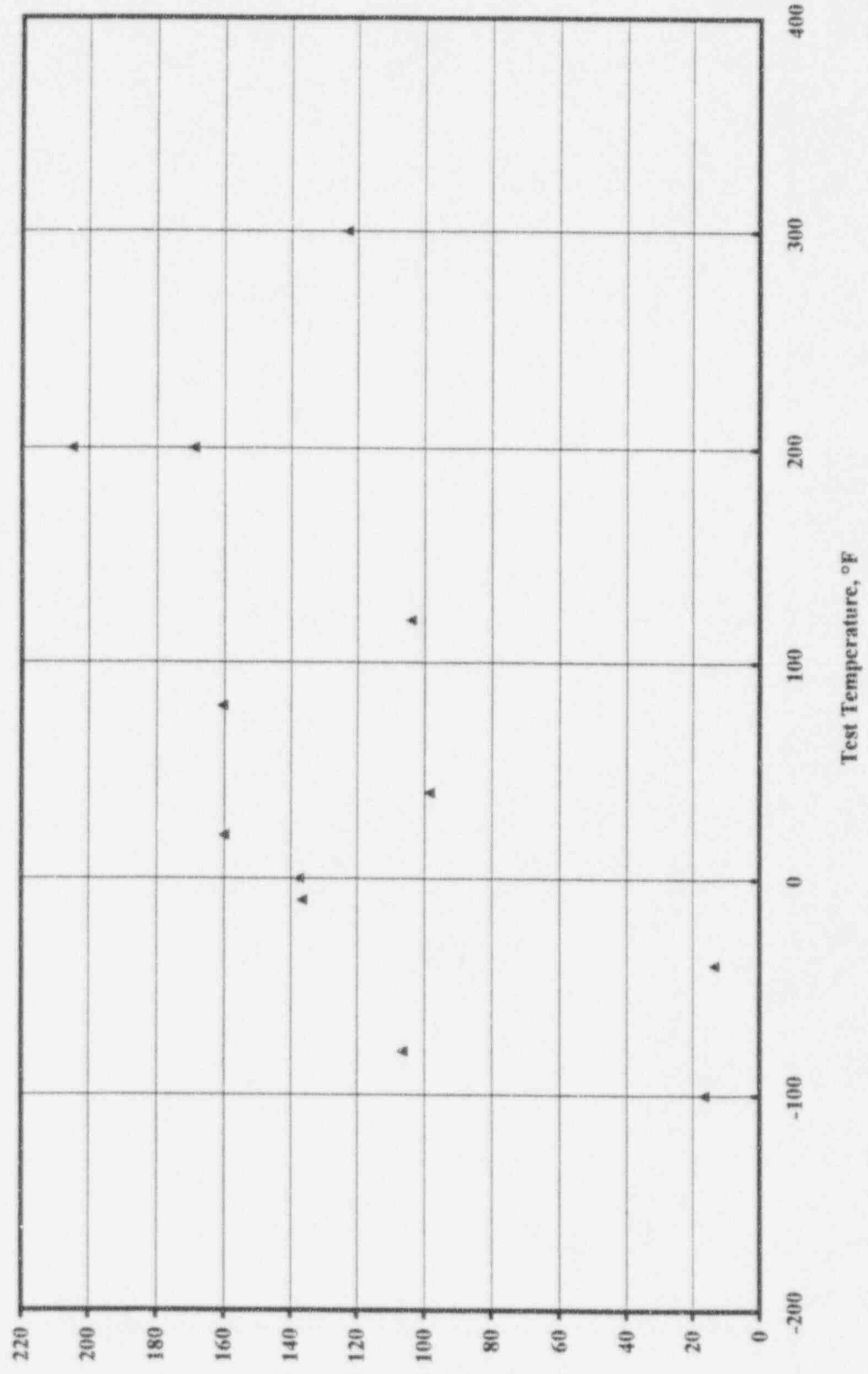

Figure 5-12. Hope Creek 1 Irradiated
HAZ Metal Impact Energy

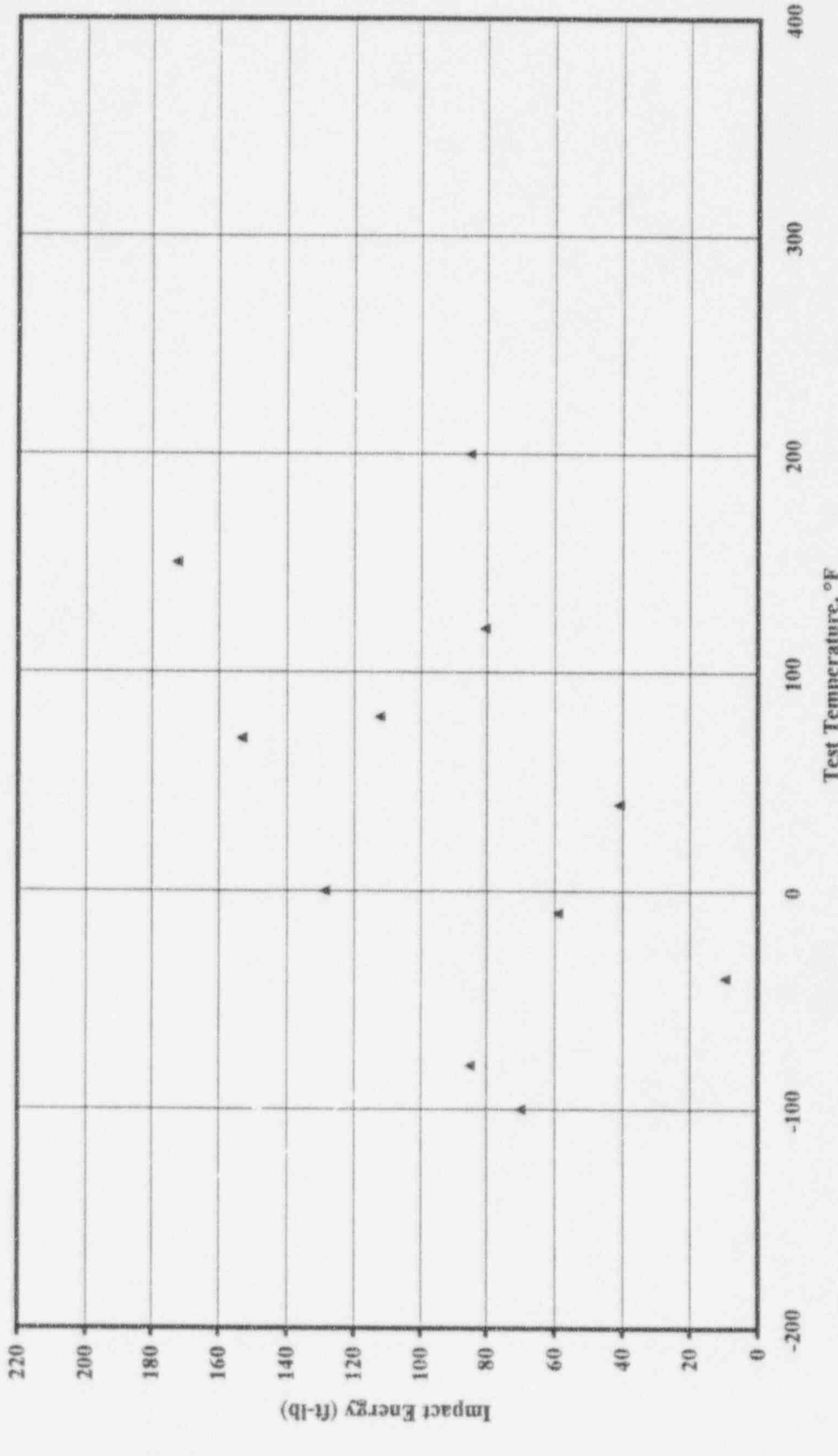

(At 300^{0}F, specimen did not entirely break for >233 ft-lb)

6. TENSILE TESTING

Six round bar tensile specimens were recovered from the surveillance capsule and sent to VNC. Uniaxial tensile tests were conducted in air at room temperature (70°F), and RPV operating temperature (550°F). Six unirradiated specimens, sent from the Hope Creek 1 site to GE-NE San Jose, were tested at the same temperatures. The tests were conducted in accordance with ASTM E8-89 [14].

6.1 PROCEDURE

All irradiated tests were conducted using a screw-driven Instron test frame equipped with a 20-kip load cell and special pull bars and grips. Heating was done with a Satec resistance clamshell furnace centered around the specimen load train. The test temperature was monitored and controlled by a chromel-alumel thermocouple spot-welded to an Inconel clip that was friction-clipped to the surface of the specimen at its midline. Before the elevated temperature tests, a profile of the furnace was conducted at the test temperature of interest using an unirradiated steel specimen of the same geometry. Thermocouples were spot-welded to the top, middle, and bottom of a central 1 inch gage of this specimen. In addition, the clip-on thermocouple was attached to the midline of the specimen. When the target temperatures of the three thermocouples were within ±5°F of each other, the temperature of the clip-on thermocouple was noted and subsequently used as the target temperature for the irradiated specimens. The tests were conducted at a calibrated crosshead speed of 0.005 in/min until well past yield, at which time the speed was increased to 0.05 inch/min until fracture. Crosshead displacement was used to monitor specimen extension during the test.

All unirradiated tests were conducted using an MTS servohydraulic testing machine equipped with a 10-kip load cell and pulling bars consistent with the configuration of the test specimens. Heating was done with a Marshall resistance clamshell furnace centered around the specimen load train. The test temperature was monitored and controlled by a chromel-alumel thermocouple attached to the test specimen. Contact extensometry was used to record the load-strain relationship for each test specimen. A strain rate of 0.005 in/in/min was used through the yield portion of the test and then increased to 0.05 in/in/min until fracture.

The test specimens were machined with a minimum diameter of 0.250 inch at the center of the gage length. The yield strength (YS) and ultimate tensile strength (UTS) were calculated by dividing the nominal area (0.0491 in^2) into the 0.2% offset load and into the maximum test load, respectively. The values listed for the uniform and total elongations were obtained from plots that recorded load versus specimen extension and are based on a 1.5 inch gage length. Reduction of area (RA) values were determined from post-test measurements of the necked specimen diameters using a calibrated blade micrometer and employing the following formula:

$$RA = 100\% * (A_o - A_f)/A_o$$

After testing, each broken specimen was photographed end-on, showing the fracture surface, and lengthwise, showing the fracture location and local necking behavior.

6.2 RESULTS

Irradiated tensile test properties of Yield Strength (YS), Ultimate Tensile Strength (UTS), Reduction of Area (RA), Uniform Elongation (UE), and Total Elongation (TE) are presented in Table 6-1; all but UE are presented in Table 6-2 for unirradiated specimens. A stress-strain curve for a 550°F base metal irradiated specimen is shown in Figure 6-1. This curve is typical of the stress-strain characteristics of all the tested specimens. The surveillance materials generally follow the trend of decreasing properties with increasing temperature. Photographs of the fracture surfaces and necking behavior are given in Figures 6-2 through 6-4.

6.3 IRRADIATED VERSUS UNIRRADIATED TENSILE PROPERTIES

The unirradiated and irradiated plate, weld, and HAZ data at room temperature and at 550°F was compared to determine the irradiation effect. In most cases, the trends of increasing YS and UTS and of decreasing TE and RA, characteristic of irradiation embrittlement, are seen in the data.

Table 6-1: TENSILE TEST RESULTS FOR IRRADIATED RPV MATERIALS

	Specimen Number	Test Temp. (°F)	Yield [a] Strength (ksi)	Ultimate Strength (ksi)	Uniform Elongation (%)	Total Elongation (%)	Reduction of Area (%)
Base:	P1A	70	70.2	91.9	9.8	17.0	68.4
	P1B	550	67.3	85.1	8.5	14.2	54.9
Weld:	P2A	70	82.2	96.0	10.3	21.0	73.1
	P2B	550	70.9	86.3	8.5	16.4	68.6
HAZ:	P3A	70	69.7	91.6	7.2	15.1	69.2
	P3B	550	66.8	86.9	6.7	14.0	67.2

[a] Yield strength is determined by 0.2% offset.

Table 6-2: TENSILE TEST RESULTS FOR UNIRRADIATED RPV MATERIALS

	Specimen Number	Test Temp. (°F)	Yield [a] Strength (ksi)	Ultimate Strength (ksi)	Total Elongation (%)	Reduction of Area (%)
Base:	26-9378	70	70.1	92.6	26.2	70.9
	26-9378	550	62.3	89.3	21.9	62.8
Weld:	26-9379	70	78.8	93.4	29.0	71.7
	26-9379	550	72.3	90.6	21.3	67.9
HAZ:	26-9380	70	68.4	91.6	19.3	68.2
	26-9380	550	62.9	88.0	16.3	60.3

[a] Yield strength is determined by 0.2% offset.

Table 6-3: COMPARISON OF UNIRRADIATED AND IRRADIATED TENSILE PROPERTIES AT ROOM TEMPERATURE

		Yield Strength (ksi)	Ultimate Strength (ksi)	Total Elongation (%)	Reduction of Area (%)
Base:	Unirradiated	70.1	92.6	26.2	70.9
	Irradiated	70.2	91.9	17.0	68.4
	Difference [a]	0.1 (0.1%)	-0.7 (-0.8%)	-9.2 (-35.1%)	-2.5 (-3.5%)
Weld:	Unirradiated	78.8	93.4	29.0	71.7
	Irradiated	82.2	96.0	21.0	73.1
	Difference [a]	3.4 (4.3%)	2.6 (2.8%)	-8.0 (-27.6%)	1.4 (2.0%)

[a] In parenthesis is %Difference = [(Irrad. - Unirrad.)/Unirrad.] * 100%

Table 6-4: COMPARISON OF UNIRRADIATED AND IRRADIATED TENSILE PROPERTIES AT 550°F

		Yield Strength (ksi)	Ultimate Strength (ksi)	Total Elongation (%)	Reduction of Area (%)
Base:	Unirradiated	62.3	89.3	21.9	62.8
	Irradiated	67.3	85.1	14.2	54.9
	Difference [a]	5.0 (8.0%)	-4.2 (-4.7%)	-7.7 (-35.2%)	-7.9 (-12.6%)
Weld:	Unirradiated	72.3	90.6	21.3	67.9
	Irradiated	70.9	86.3	16.4	68.6
	Difference [a]	-1.4 (-1.9%)	-4.3 (-4.7%)	-4.9 (-23.0%)	0.7 (1.0%)

[a] In parenthesis is %Difference = [(Irrad. - Unirrad.)/Unirrad.] * 100%

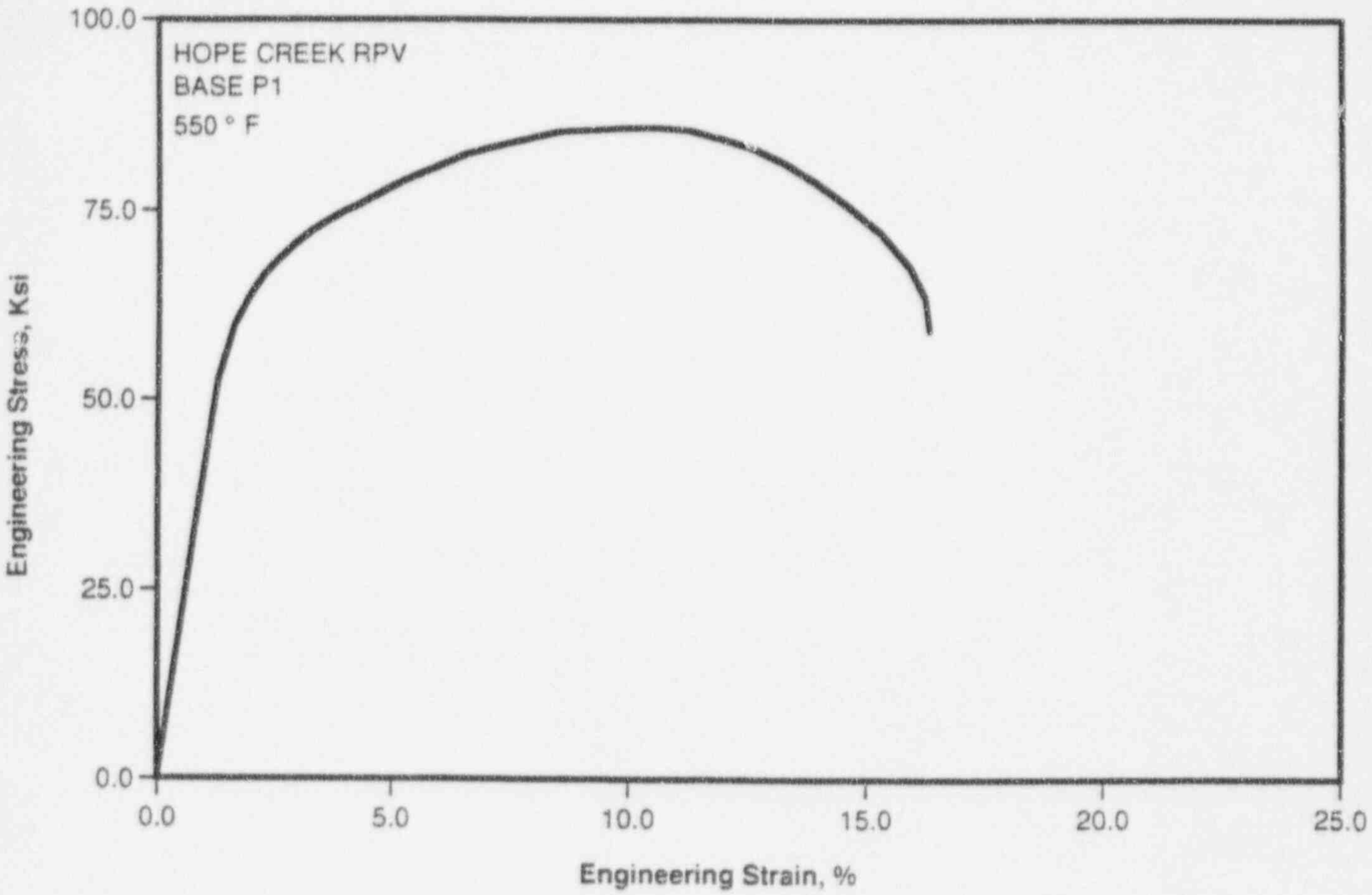

Figure 6-1. Typical Engineering Stress-Strain for Irradiated RPV Materials

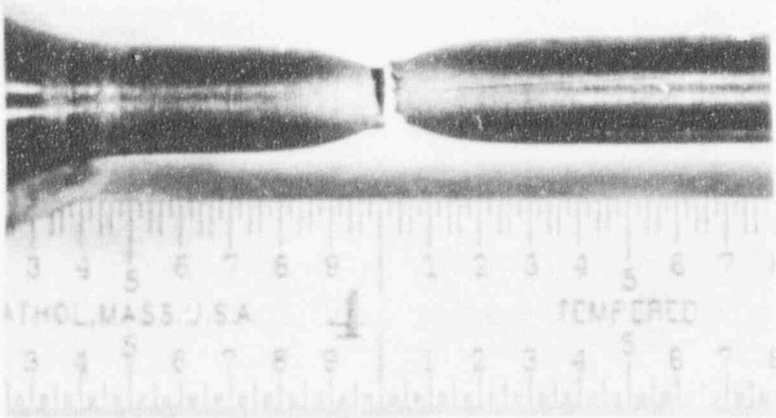

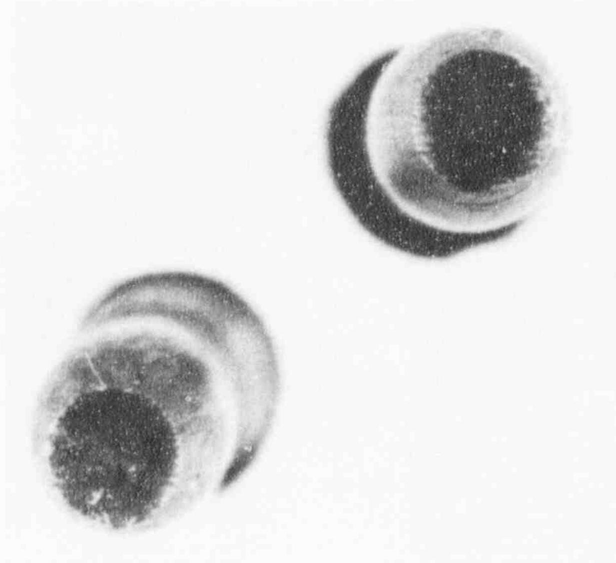

P1A 70°F

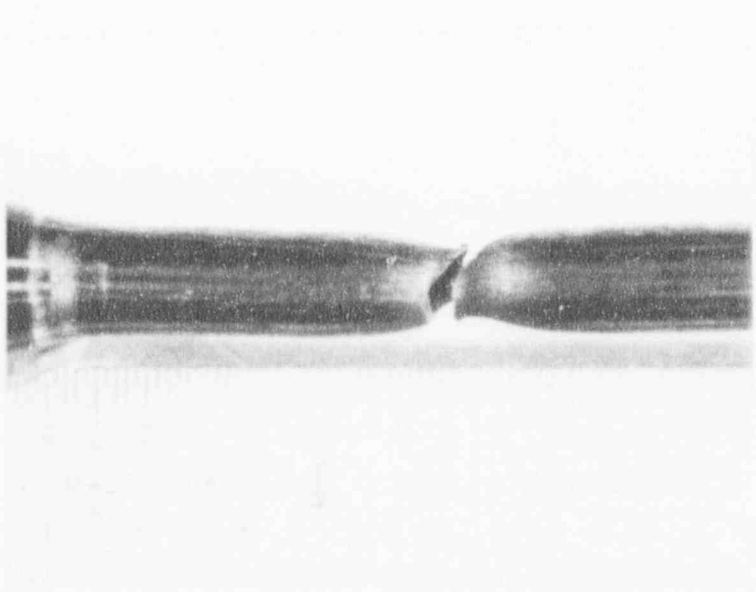

P1B 550°F

Figure 6-2 Fracture Location, Necking Behavior and Fracture Appearance for Irradiated Base Metal Tensile Specimens

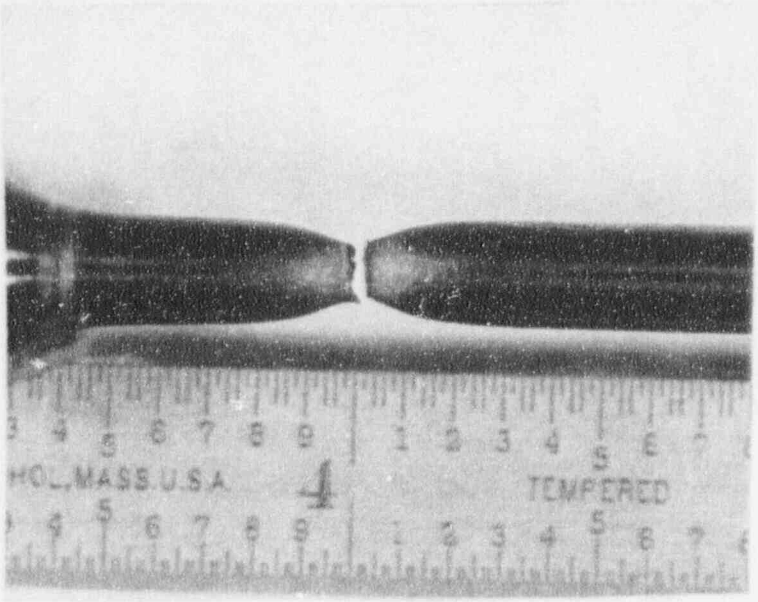

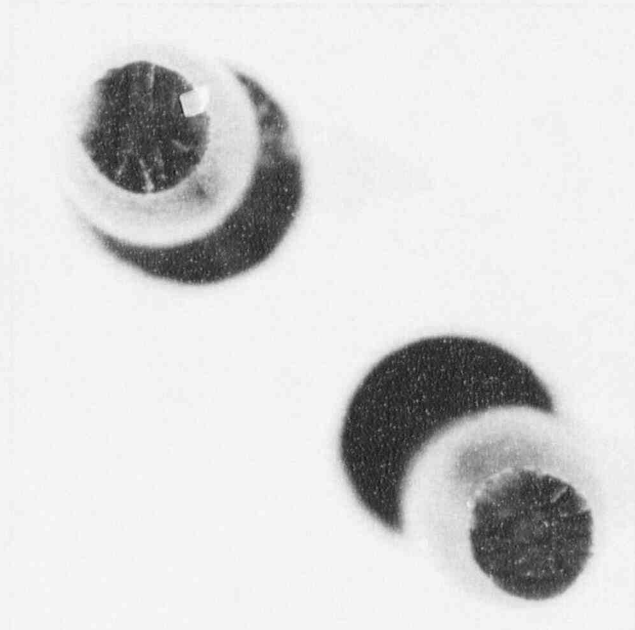

P2A

70°F

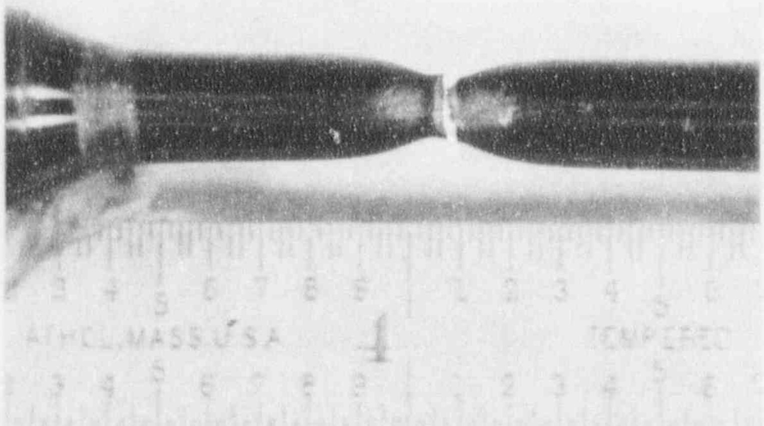

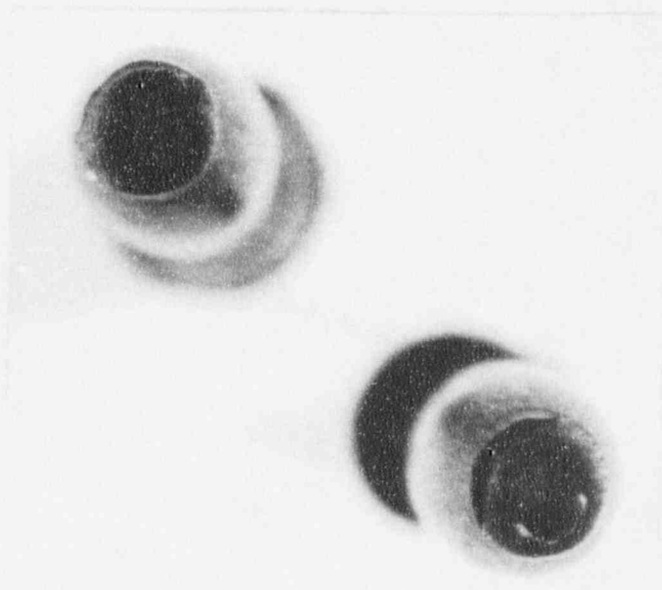

P2B

550°F

Figure 6-3. Fracture Location, Necking Behavior and Fracture Appearance for Irradiated Weld Metal Tensile Specimens

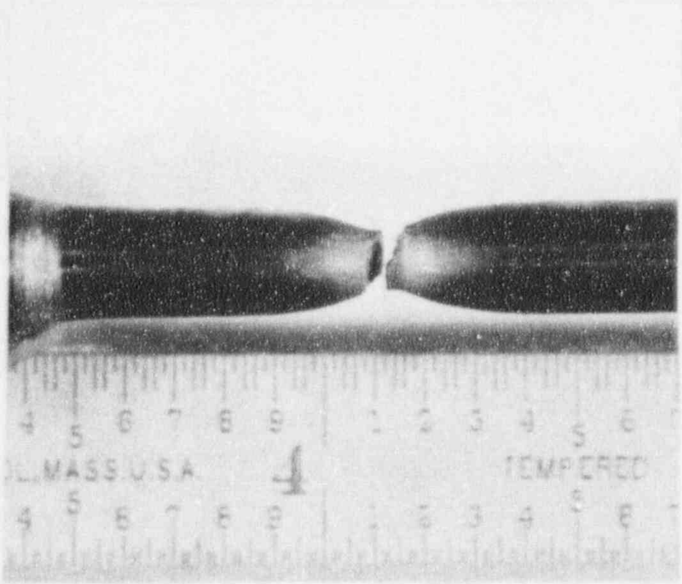

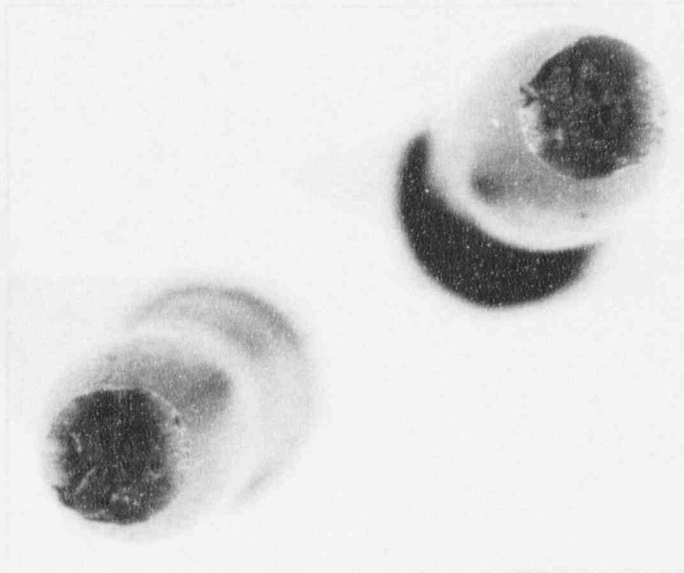

P3A 70°F

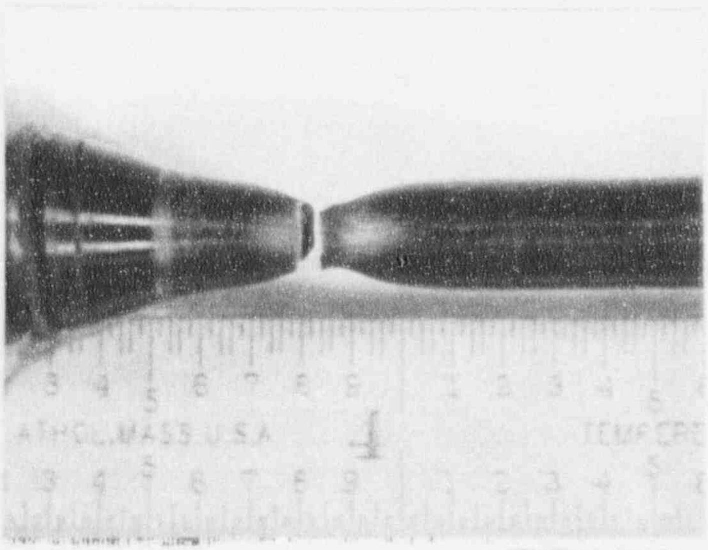

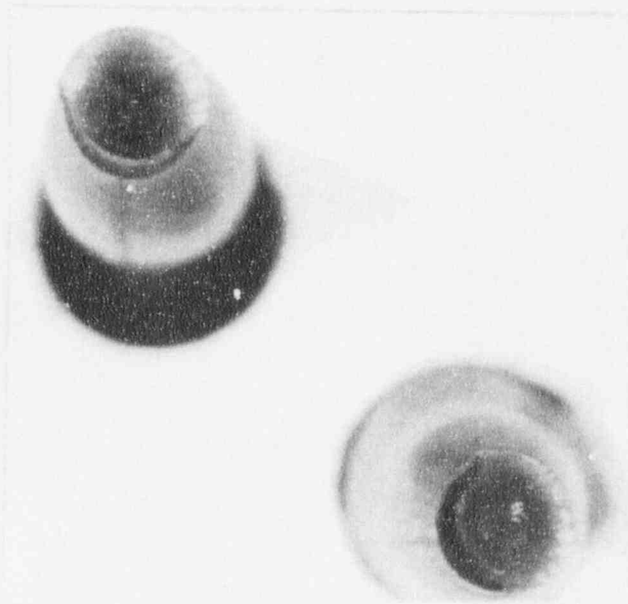

P3B 550°F

Figure 6-4. Fracture Location, Necking Behavior and Fracture Appearance for Irradiated HAZ Metal Tensile Specimens

7. DEVELOPMENT OF OPERATING LIMITS CURVES

The aspects of the curves which have changed as a result of the testing presented here and as a result of ASME Code changes are discussed below.

7.1 BACKGROUND

The revised fluence values in Section 4, which are about 14% greater than the current nominal fluence value, is used in this section to revise the adjusted reference temperatures (ARTs), which are then used to revise the beltline P-T curves.

The P-T curve revision includes consideration of the change to the allowable fracture toughness equation in ASME Code Section XI, Appendix G, which occurred in 1992. The coefficient 1.233 in the K_{IR}/K_{Ia} equation in Figure G-2210-1, became 1.223. The revision adds about 1/2°F to the calculated temperature for a given pressure on the P-T curves (i.e., all curved portions of the P-T curves shift 1/2°F to the right). The resulting P-T curves for pressure tests (Curve A), non-nuclear heatup/cooldown (Curve B) and core-critical operation (Curve C) are shown in Figures 7-1 through 7-3, respectively. The P-T limits are provided in tabular form in Table 7-1.

7.2 NON-BELTLINE REGIONS

The non-beltline curves are developed for two regions: the upper vessel region, governed by the feedwater nozzle limits, and the bottom head region, governed by the CRD penetration limits. Table 3-2 has these limiting initial RT_{NDT} values which are: 40°F for the upper vessel region, based on the feedwater nozzle (a value of 40°F consistent with the purchase specification was used, since initial RT_{NDT} values were unavailable for many of the vessel nozzles) and 30°F for the bottom head region, based on the bottom head. The 1/2°F adjustment was made to the curved portions of the non-beltline curves, but not to the straight line and step portions, which are based on 10CFR50 Appendix G.

Although bottom head Curve B is not limiting, it is included in Figure 7-2, as there may be transients where the bottom head is cooler than the upper vessel regions.

7.3 CORE BELTLINE REGION

Figures 7-1 through 7-3 show the beltline curves at 32 EFPY. As with the non-beltline curves, the 1/2°F adjustment was made to the curved portions of the beltline curves.

7.4 EVALUATION OF IRRADIATION EFFECTS

The impact on adjusted reference temperature (ART) due to irradiation in the beltline materials is determined according to the methods in Reg. Guide 1.99 [7], as a function of neutron fluence and the element contents of copper (Cu) and nickel (Ni). The specific relationship from Reg. Guide 1.99 [7] is:

$$ART = \text{Initial } RT_{NDT} + \Delta RT_{NDT} + \text{Margin} \quad (7\text{-}1)$$

where:

$$\Delta RT_{NDT} = [CF]*f^{(0.28 - 0.10 \log f)} \quad (7\text{-}2)$$

$$\text{Margin} = 2*(\sigma_I^2 + \sigma_\Delta^2)^{1/2} \quad (7\text{-}3)$$

CF = chemistry factor from Tables 1 or 2 of Reg. Guide 1.99 [7],

f = 1/4 T fluence (n/cm^2) divided by 10^{19},

σ_I = standard deviation on initial RT_{NDT},

σ_Δ = standard deviation on ΔRT_{NDT}, is 28°F for welds and 17°F for base material, except that σ_Δ need not exceed 0.50 times the ΔRT_{NDT} value.

Once two sets of surveillance capsule data are available, the CF values in Reg. Guide 1.99 [7] can be modified to reflect the results. However, this is only the first set of surveillance data from Hope Creek 1, so only the results of the flux wire tests are factored into beltline ART calculations.

Each beltline plate and weld ΔRT_{NDT} value is determined by multiplying the CF from Reg. Guide 1.99, determined for the Cu-Ni content of the material, by the fluence factor for the EFPY being evaluated. The Margin term and initial RT_{NDT} are added to get the ART of the material. The 32 EFPY ART values are shown in Table 7-2. Results for all of the beltline plates and several of the most limiting beltline welds are shown.

The LPCI nozzle is partially in the beltline region; its value of initial RT_{NDT} is -20°F per Table 3-2. Comparing the ART of the LPCI nozzle (24.3°F), determined in Table 7-2, with an initial RT_{NDT} for non-beltline nozzles of 40°F, the non-beltline nozzles are more limiting and are used to develope the P-T curves.

7.4.1 ART Versus EFPY

The results in Table 7-2 show that beltline plate 5K3025/1 is limiting at 32 EFPY; the most limiting weld is D53040/1125-02205. Figure 7-4 shows the ART as a function of EFPY for the most limiting plate and weld. The resulting ARTs at 32 EFPY are 72.5°F for the plate and 32.8°F for the weld.

7.4.2 Upper Shelf Energy at 32 EFPY

Paragraph IV.B of 10CFR50 Appendix G [1] sets limits on the upper shelf energy (USE) of the beltline materials. The USE must be above 50 ft-lb at all times during plant operation, assumed here to be up to 32 EFPY. Calculations of 32 EFPY USE, using Reg. Guide 1.99 [7] methods, are summarized in Table 7-3. Percent decrease in USE as a function of fluence and copper content is shown in Figure 2 of Reg. Guide 1.99. Therefore, the values of 32 EFPY fluence at 1/4 T location as determined in Section 4.3 along with the copper content of the beltline materials listed in Table 3-1 provide the necessary information to determine percent decrease in USE. The initial USE of the beltline plates and welds were obtained from Table 5A-19 of Reference [5]. The unirradiated surveillance plate and weld data from Table 5-4 are also included for comparison.

From Table 7-3, the lowest value of 32 EFPY USE for the beltline plate is 67 ft-lb. Information in [5] indicates that the specimens data were for transverse orientation.

Weld metal initial USE values were taken during vessel fabrication at 10°F for all heats. Unlike the plate, the weld metal USE has no transverse/longitudinal correction because weld metal has no orientation effect. The lowest weld USE at 32 EFPY, as shown in Table 7-3, is 60 ft-lb, which is expected to be quite conservative based on initial data at 10°F.

Based on the above results, it is expected that the beltline materials will have USE values above 50 ft-lb at 32 EFPY, as required in 10CFR50 Appendix G [1]. Since USE and ART requirements are met, irradiation effects are not severe enough to necessitate additional analyses or preparations for RPV annealing before 32 EFPY. Moreover, PSE&G is a participant in a BWR Owners' Group program to perform analyses to demonstrate equivalent margin in cases where the USE drops below 50 ft-lb [18]. This analysis shows equivalent margin at USE values as low as 35 ft-lb. The calculations in Tables B-1 and B-2 in Appendix B show that the equivalent margin analysis is applicable.

7.5 OPERATING LIMITS CURVES VALID TO 32 EFPY

Figures 7-1 through 7-3 show P-T curves valid to 32 EFPY. The P-T curves are developed by considering the requirements applicable to the non-beltline, beltline, and closure flange regions. For most of each curve, the beltline curves are more limiting. The bottom head has been included on Curve B to provide the appropriate limits for transients where some bottom head stratification might occur.

Table 7-1
HOPE CREEK 1 P-T CURVE VALUES

PRESSURE	32 EFPY BELTLINE CURVE A	NON-BELTLINE CURVE A	BOTTOM HEAD CURVE B	32 EFPY BELTLINE CURVE B	UPPER VESSEL CURVE B	NON-BELTLINE CURVE B	32 EFPY BELTLINE CURVE C	NON-BELTLINE CURVE C
	*****************	REQUIRED	TEMPERATURES	*****************				
0		79.0			79.0	79.0		79.0
10		79.0			79.0	79.0		79.0
20		79.0			79.0	79.0		79.0
30		79.0			79.0	79.0		79.0
40		79.0			79.0	79.0		80.6
50		79.0			79.0	79.0		93.6
60		79.0			79.0	79.0		104.6
70		79.0			79.0	79.0		114.1
80		79.0			82.3	82.3		122.3
90		79.0			89.3	89.3		129.3
100		79.0			95.4	95.4		135.4
110		79.0			101.0	101.0		141.0
120		79.0			105.9	105.9		145.9
130		79.0			110.7	110.7		150.7
140		79.0			115.3	115.3		155.3
150		79.0			119.6	119.6		159.6
160		79.0			123.5	123.5		163.5
170		79.0			126.9	126.9		166.9
180		79.0			129.9	129.9		169.9
190		79.0			132.7	132.7		172.7
200		79.0			135.4	135.4	69.6	175.4
210		79.0			138.1	138.1	78.9	178.1
220		79.0			140.6	140.6	87.0	180.6
230		79.0			143.0	143.0	94.4	183.0
240		79.0			145.3	145.3	101.0	185.3
250		79.0			147.5	147.5	107.0	187.5
260		79.0			149.6	149.6	112.6	189.6
270		79.0			151.6	151.6	117.7	191.6
280		79.0			153.6	153.6	122.5	193.6
290		79.0			155.5	155.5	126.9	195.5
300		79.0		94.2	157.3	157.3	134.2	197.3
310		79.0		98.1	159.1	159.1	138.1	199.1
312.5		79.0		99.0	159.5	159.5	139.0	199.5
312.5		109.0		99.0	159.5	159.5	139.0	199.5
320		109.0		101.7	160.8	160.8	141.7	200.8
330		109.0		105.2	162.4	162.4	145.2	202.4
340		109.0		108.5	164.0	164.0	148.5	204.0
350		109.0		111.7	165.6	165.6	151.7	205.6
360		109.0		114.7	167.1	167.1	154.7	207.1
370		109.0		117.6	168.6	168.6	157.6	208.6
380		109.0		120.4	170.1	170.1	160.4	210.1
390		109.0		123.1	171.6	171.6	163.1	211.6
400		109.0	60.6	125.7	173.1	173.1	165.7	213.1
410		109.0	69.6	128.1	174.6	174.6	168.1	214.6
420		109.0	76.6	130.5	176.0	176.0	170.5	216.0
430		109.0	82.6	132.8	177.4	177.4	172.8	217.4
440		109.0	87.6	135.1	178.8	178.8	175.1	218.8
450		109.0	91.6	137.3	180.1	180.1	177.3	220.1
460		109.0	95.1	139.4	181.4	181.4	179.4	221.4
470		109.0	98.2	141.4	182.7	182.7	181.4	222.7
480		109.0	101.1	143.4	183.9	183.9	183.4	223.9

Table 7-1
HOPE CREEK 1 P-T CURVE VALUES

PRESSURE	32 EFPY BELTLINE CURVE A	NON-BELTLINE CURVE A	BOTTOM HEAD CURVE B	32 EFPY BELTLINE CURVE B	UPPER VESSEL CURVE B	NON-BELTLINE CURVE B	32 EFPY BELTLINE CURVE C	NON-BELTLINE CURVE C
	REQUIRED TEMPERATURES							
490		109.0	103.9	145.3	185.1	185.1	185.3	225.1
500	69.6	109.0	106.6	147.2	186.3	186.3	187.2	226.3
510	73.7	109.0	109.3	149.0	187.4	187.4	189.0	227.4
520	77.6	109.0	111.9	150.8	188.5	188.5	190.8	228.5
530	81.3	109.0	114.5	152.5	189.6	189.6	192.5	229.6
540	84.8	109.0	117.0	154.2	190.6	190.6	194.2	230.6
550	88.2	109.0	119.4	155.9	191.6	191.6	195.9	231.6
560	91.4	109.0	121.7	157.5	192.6	192.6	197.5	232.6
570	94.4	109.0	123.9	159.0	193.5	193.5	199.0	233.5
580	97.3	109.0	126.0	160.6	194.4	194.4	200.6	234.4
590	100.1	109.0	127.8	162.1	195.3	195.3	202.1	235.3
600	102.8	109.0	129.6	163.6	196.1	196.1	203.6	236.1
610	105.4	109.0	131.3	165.0	196.9	196.9	205.0	236.9
620	107.9	109.0	133.1	166.4	197.7	197.7	206.4	237.7
• 625	109.1	109.0	133.9	167.1	198.0	198.0	207.1	238.0
630	110.3	109.0	134.7	167.8	198.4	198.4	207.8	238.4
640	112.7	109.0	136.4	169.2	199.1	199.1	209.2	239.1
650	114.9	109.0	137.9	170.5	199.7	199.7	210.5	239.7
660	117.1	109.0	139.4	171.8	200.4	200.4	211.8	240.4
670	119.2	110.2	140.9	173.1	201.0	201.0	213.1	241.0
680	121.2	112.0	142.4	174.[illegible]	201.5	201.5	214.3	241.5
690	123.2	113.8	143.8	175.6	202.1	202.1	215.6	242.1
700	125.2	115.6	145.2	176.8	202.6	202.6	216.8	242.6
710	127.1	117.3	146.6	178.0	203.1	203.1	218.0	243.1
720	128.9	118.9	147.9	179.2	203.5	203.5	219.2	243.5
730	130.7	120.6	149.2	180.3	204.0	204.0	220.3	244.0
740	132.4	122.1	150.4	181.5	204.4	204.4	221.5	244.4
750	134.1	123.7	151.6	182.6	204.9	204.9	222.6	244.9
760	135.8	125.2	152.7	183.7	205.3	205.3	223.7	245.3
770	137.4	126.7	153.8	184.7	205.7	205.7	224.7	245.7
780	139.0	128.1	154.9	185.8	206.1	206.1	225.8	246.1
790	140.5	129.6	156.0	186.9	206.5	206.5	226.9	246.5
800	142.0	130.9	157.1	187.9	206.9	206.9	227.9	246.9
810	143.5	132.3	158.2	188.9	207.3	207.3	228.9	247.3
820	144.9	133.6	159.3	189.9	207.7	207.7	229.9	247.7
830	146.4	134.9	160.3	190.9	208.1	208.1	230.9	248.1
840	147.8	136.2	161.4	191.9	208.4	208.4	231.9	248.4
850	149.1	137.5	162.4	192.8	208.8	208.8	232.8	248.8
860	150.5	138.7	163.5	193.8	209.1	209.1	233.8	249.1
870	151.8	139.9	164.5	194.7	209.5	209.5	234.7	249.5
880	153.0	141.1	165.6	195.6	209.8	209.8	235.6	249.8
890	154.3	142.3	166.6	196.6	210.2	210.2	236.6	250.2
900	155.6	143.4	167.7	197.4	210.5	210.5	237.4	250.5
910	156.8	144.6	168.7	198.3	210.8	210.8	238.3	250.8
920	158.0	145.7	169.7	199.2	211.2	211.2	239.2	251.2
930	159.1	146.8	170.7	200.1	211.5	211.5	240.1	251.5
940	160.3	147.8	171.7	200.9	211.9	211.9	240.9	251.9
950	161.4	148.9	172.7	201.8	212.2	212.2	241.8	252.2
960	162.6	149.9	173.7	202.6	212.5	212.5	242.6	252.5
970	163.7	151.0	174.7	203.4	212.9	212.9	243.4	252.9
980	164.7	152.0	175.7	204.2	213.2	213.2	244.2	253.2

Table 7-1
HOPE CREEK 1 P-T CURVE VALUES

***********************************REQUIRED TEMPERATURES****************************

PRESSURE	32 EFPY BELTLINE CURVE A	NON-BELTLINE CURVE A	BOTTOM HEAD CURVE B	32 EFPY BELTLINE CURVE B	UPPER VESSEL CURVE B	NON-BELTLINE CURVE B	32 EFPY BELTLINE CURVE C	NON-BELTLINE CURVE C
990	165.8	153.0	176.6	205.0	213.6	213.6	245.0	253.6
1000	166.9	153.9	177.6	205.8	213.9	213.9	245.8	253.9
1010	167.9	154.9	178.5	206.6	214.2	214.2	246.6	254.2
1020	168.9	155.9	179.4	207.4	214.6	214.6	247.4	254.6
1030	169.9	156.8	180.2	208.2	214.9	214.9	248.2	254.9
1040	170.9	157.7	181.0	208.9	215.2	215.2	248.9	255.2
1050	171.9	158.6	181.8	209.7	215.6	215.6	249.7	255.6
1060	172.8	159.5	182.6	210.4	215.9	215.9	250.4	255.9
1070	173.8	160.4	183.4	211.2	216.2	216.2	251.2	256.2
1080	174.7	161.3	184.2	211.9	216.5	216.5	251.9	256.5
1090	175.7	162.2	184.9	212.6	216.9	216.9	252.6	256.9
1100	176.6	163.0	185.7	213.3	217.2	217.2	253.3	257.2
1110	177.5	163.9	186.4	214.0	217.5	217.5	254.0	257.5
1120	178.4	164.7	187.1	214.7	217.9	217.9	254.7	257.9
1130	179.2	165.5	187.8	215.4	218.2	218.2	255.4	258.2
1140	180.1	166.3	188.5	216.1	218.5	218.5	256.1	258.5
1150	181.0	167.1	189.2	216.8	218.9	218.9	256.8	258.9
1160	181.8	167.9	189.9	217.4	219.2	219.2	257.4	259.2
1170	182.6	168.7	190.6	218.1	219.5	219.5	258.1	259.5
1180	183.5	169.5	191.2	218.8	219.8	219.8	258.8	259.8
1190	184.3	170.2	191.9	219.4	220.1	220.1	259.4	260.1
1200	185.1	171.0	192.6	220.1	220.4	220.4	260.1	260.4
1210	185.9	171.7	193.2	220.7	220.8	220.8	260.7	260.8
* 1215	186.3	172.1	193.5	221.0	220.9	220.9	261.0	260.9
1220	186.7	172.5	193.9	221.3	221.1	221.1	261.3	261.1
1230	187.4	173.2	194.5	222.0	221.4	221.4	262.0	261.4
1240	188.2	173.9	195.2	222.6	221.7	221.7	262.6	261.7
1250	189.0	174.7	195.8	223.2	222.0	222.0	263.2	262.0
1260	189.7	175.4	196.5	223.8	222.3	222.3	263.8	262.3
1270	190.5	176.1	197.1	224.4	222.6	222.6	264.4	262.6
1280	191.2	176.8	197.8	225.0	223.0	223.0	265.0	263.0
1290	191.9	177.4	198.4	225.6	223.3	223.3	265.6	263.3
1300	192.7	178.1	199.1	226.2	223.6	223.6	266.2	263.6
1310	193.4	178.8	199.7	226.8	223.9	223.9	266.8	263.9
1320	194.1	179.5	200.4	227.4	224.2	224.2	267.4	264.2
1330	194.8	180.1	201.0	228.0	224.5	224.5	268.0	264.5
1340	195.5	180.8	201.7	228.5	224.8	224.8	268.5	264.8
1350	196.2	181.4	202.3	229.1	225.1	225.1	269.1	265.1
1360	196.8	182.1	203.0	229.7	225.4	225.4	269.7	265.4
1370	197.5	182.7	203.6	230.2	225.7	225.7	270.2	265.7
1380	198.2	183.3	204.3	230.8	226.0	226.0	270.8	266.0
1390	198.8	183.9	204.9	231.3	226.3	226.3	271.3	266.3
1400	199.5	184.6	205.6	231.9	226.6	226.6	271.9	266.6

* Values linearly interpolated. Curves A intersect at approximately 625 psig. Curves B (except Bottom Head) intersect at approximately 1215 psig, and Curves C intersect at approximately 1215 psig.

Table 7-2
BELTLINE ART VALUES FOR HOPE CREEK 1

Shell Course #3 Plate and Weld 3/4
Thickness = 6.1 inches

Shell Course #4 & 5 and Welds4/5
Thickness = 6.1 inches

LPCI Nozzle and Weld
Thickness = 6.1 inches

Shell Course #3 Plate and Weld 3/4
32 EFPY Peak I.D. fluence = 4.94E+17
32 EFPY Peak 1/4 T fluence = 3.42E+17

Shell Course #4 & 5 and Welds4/5
32 EFPY Peak I.D. fluence = 7.50E+17
32 EFPY Peak 1/4 T fluence = 5.20E+17

LPCI Nozzle and Weld
32 EFPY Peak I.D. fluence = 4.05E+17
32 EFPY Peak 1/4 T fluence = 2.81E+17

COMPONENT	I.D. or Type	HEAT OR HEAT/LOT	%Cu	%Ni	CF	Initial RTndt °F	32 EFPY Delta RTndt °F	Margin °F	32 EFPY Shift °F	32 EFPY ART °F
PLATES:										
Lower	No. 5	5K3230 / 1	0.07	0.56	44	-10.0	13.2	13.2	26.3	16.3
	No. 5	6C35 / 1	0.09	0.54	58	-11.0	17.3	17.3	34.7	23.7
	No. 5	6C45 / 1	0.08	0.57	51	1.0	15.2	15.2	30.5	31.5
Lower-Intmed	No. 4	5K2963 / 1	0.07	0.58	44	-10.0	13.2	13.2	26.3	16.3
	No. 4	5K2530 / 1	0.08	0.56	51	19.0	15.2	15.2	30.5	49.5
	No. 4	5K3238 / 1	0.09	0.64 *	58	7.0	17.3	17.3	34.7	41.7
Intermediate	No. 3	5K3025 / 1	0.15	0.71	113	19.0	26.7	26.7	53.5	72.5
	No. 3	5K2608 / 1	0.09	0.58	58	19.0	13.7	13.7	27.5	46.5
	No. 3	5K2698 / 1	0.10	0.58	65	19.0	15.4	15.4	30.8	49.8
LPCI Nozzle	N7	19468 / 1	0.12	0.80	86	-20.0	18.2	18.2	36.3	16.3
	N7	10024 / 1	0.14	0.82	105	-20.0	22.2	22.2	44.3	24.3
VERTICAL WELDS 4/5:	SMAW	510-01205	0.09	0.54	109	-40.0	32.6	32.6	65.2	25.2
	SAW	D53040/1125-02205	0.08	0.59 *	105	-30.0	31.4	31.4	62.8	32.8
LPCI NOZZLE WELDS:	SMAW	001-01205	0.02	0.51	27	-40.0	5.7	5.7	11.4	-28.6
GIRTH WELD: 3/4:	SMAW	519-01205	0.01	0.53	20	-49.0	4.7	4.7	9.5	-39.5
	SMAW	504-01205	0.01	0.51	20	-31.0	4.7	4.7	9.5	-21.5
	SAW	D53040/1810-02205	0.10	0.68	126	-49.0	29.9	29.9	59.7	10.7
	SAW	D55733/1810-02205	0.10	0.68	126	-40.0	29.9	29.9	59.7	19.7

Note: Data of Cu and Ni wt% and initial RTndt are taken from HCGS-UFSAR.
* Average % Cu and %Ni from Table 3-3 is used.

Table 7-3.

UPPER SHELF ENERGY ANALYSIS FOR HOPE CREEK 1 BELTLINE MATERIAL

LOCATION	HEAT	INITIAL.[a] TRANS. USE	%Cu	%DECR.[b] USE	32 EFPY TRANS. USE
PLATES:					
Lower	5K3230/1	121	0.07	8	111
	6C35/1	107	0.09	9	97
	6C45/1	97	0.08	8.5	89
Low-Int.	5K2963/1	102	0.07	8	94
	5K2530/1	86	0.08	8.5	79
	5K3238/1	76	0.09	9	69
Unirradiated [c] Surveillance	5K3238/1	91	0.09	9	83
Int.	5K3025/1	75	0.15	11	67
	5K2608/1	75	0.09	8	69
	5K2698/1	75	0.10	8.5	69
LPCI Nozzle					
	19468/1	>79	0.12	9	72
	10024/1	>70	0.14	10	63
WELD:					
Vertical	510-01205	>92.5	0.09	11.5	82
	D53040	135	0.08	11	120
Unirradiated [c] Surveillance	D53040	164	0.08	11	146
LPCI Nozzle	001-01205	>109	0.02	6	102
Girth	519-01205	>109	0.01	5	104
	504-01205	>125	0.01	5	119
	D53040	>95	0.10	11	85
	D55733	>68	0.10	11	60

[a] Initial USE obtained from HCGS-UFSAR. Transverse plate values are conservatively estimated as described in the UFSAR; test temperatures for plate materials were not available. Weld values are conservatively based on data taken at 10°F.

[b] Values obtained from Figure 2 of [7] for 32 EFPY 1/4 T fluences equal to $5.2x10^{17}$ n/cm^2, for Low. and Low-Int. shells; $3.42x10^{17}$ n/cm^2, for Int. shell; and $2.81x10^{17}$ n/cm^2, for LPCI Nozzle. A fluence of $5.2x10^{17}$ n/cm^2 was used for the welds identified as vertical and $3.42x10^{17}$ n/cm^2 for the welds identified as girth.

[c] USE data taken from Table 5-4 and chemistry data from Table 3-3

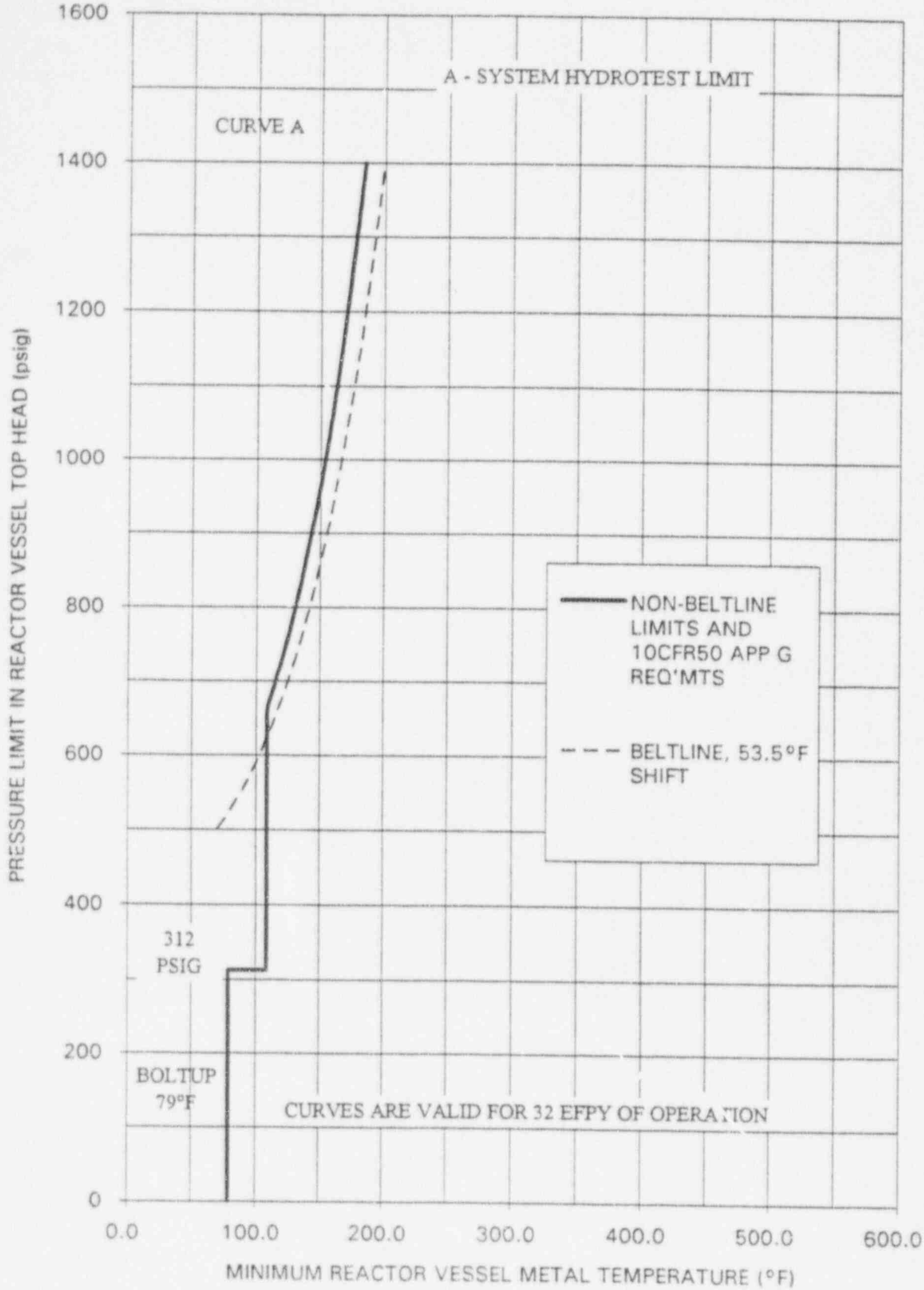

Figure 7-1. Pressure Test P-T Curves for Hope Creek 1

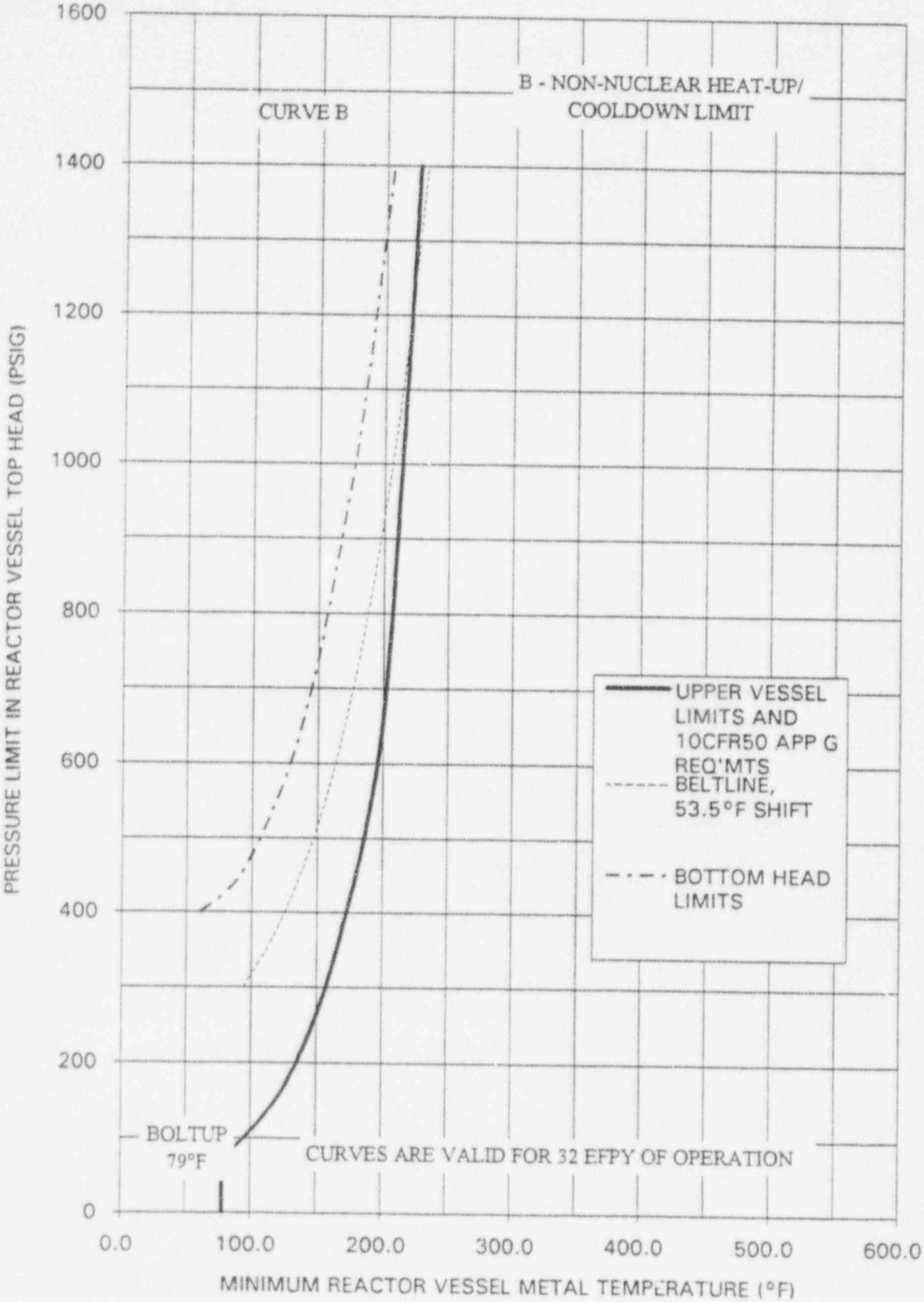

Figure 7-2. Heatup/Cooldown P-T Curves for Hope Creek 1

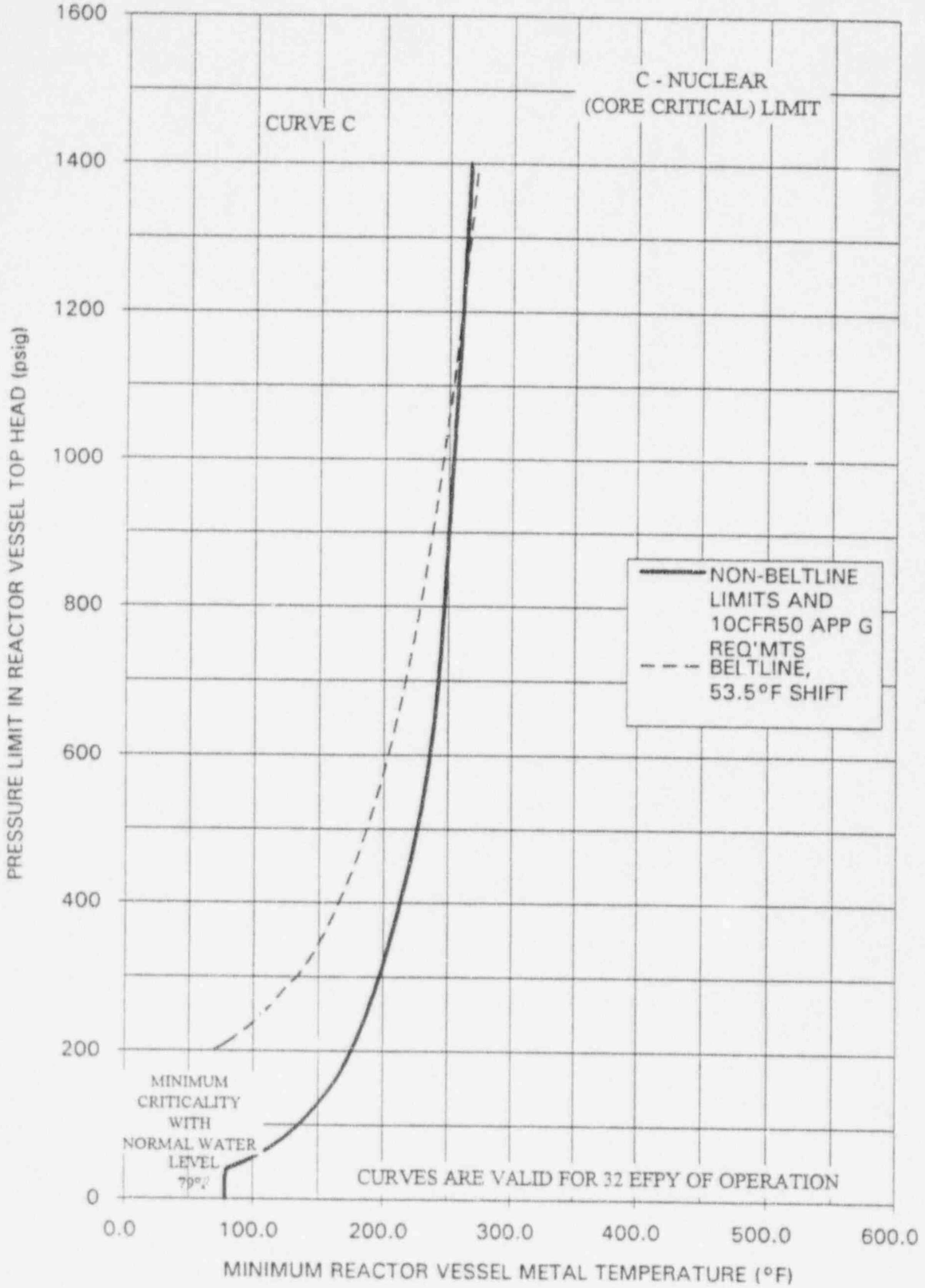

Figure 7-3. Core Critical Operation P-T Curves for Hope Creek 1

Figure 7-4. ART of Limiting Beltline Plate and Weld Materials

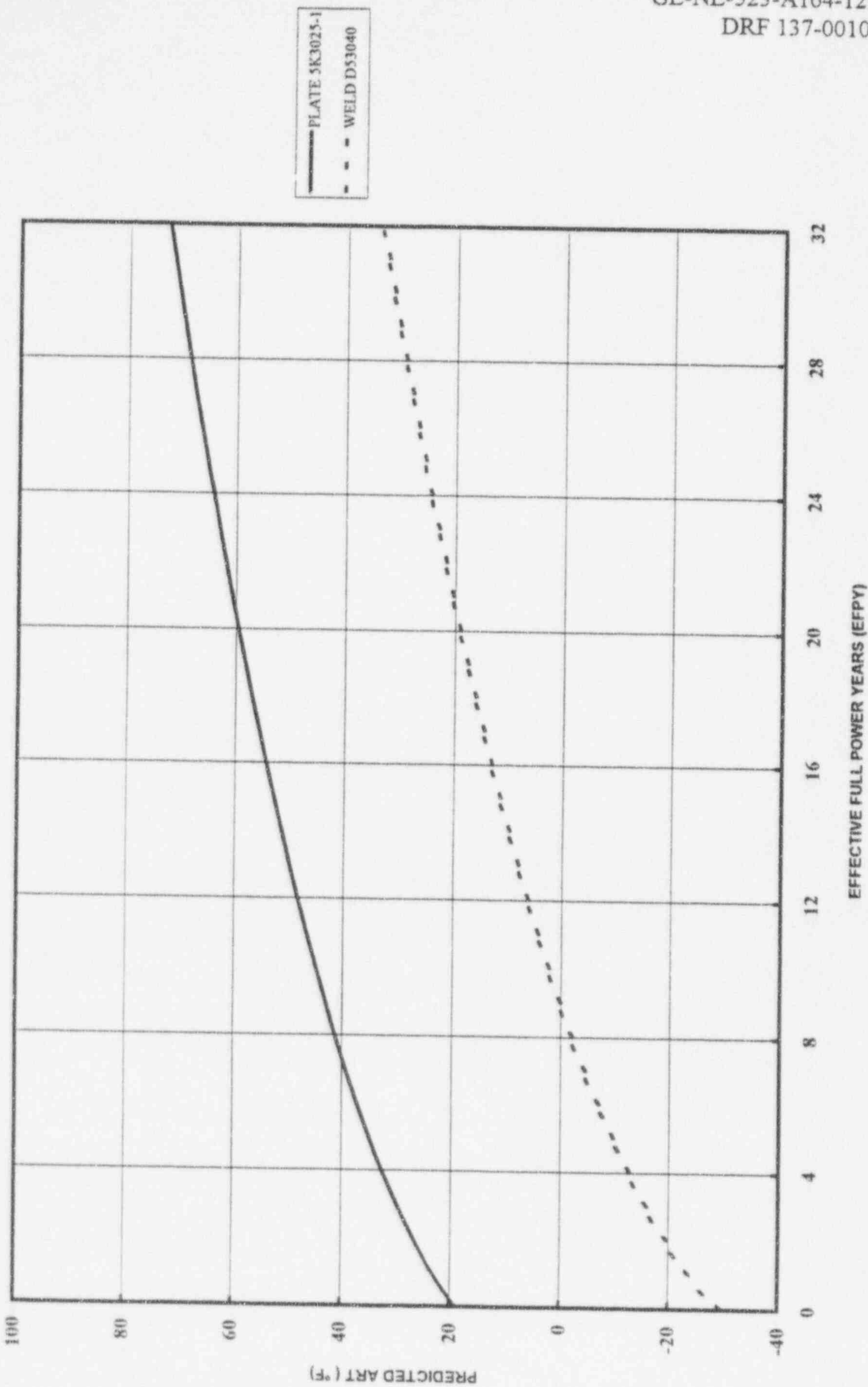

8. REFERENCES

[1] "Fracture Toughness Requirements," Appendix G to Part 50 of Title 10 of the Code of Federal Regulations, May 1983.

[2] "Protection Against Non-Ductile Failure," Appendix G to Section XI of the 1992 ASME Boiler & Pressure Vessel Code.

[3] "Reactor Vessel Material Surveillance Program Requirements," Appendix H to Part 50 of Title 10 of the Code of Federal Regulations, May 1983.

[4] "Surveillance Test for Nuclear Reactor Vessels," ASTM E185-66

[5] Hope Creek Generating Station Updated Final Safety Analysis Report, Section 5.3

[6] "Conducting Surveillance Tests for Light Water Cooled Nuclear Power Reactor Vessels," Annual Book of ASTM Standards, E185-82, July 1982.

[7] "Radiation Embrittlement of Reactor Vessel Materials," USNRC Regulatory Guide 1.99, Revision 2, May 1988.

[8] "Location and Numbering of Surveillance Test Specimens", Babcock-Hitachi (Drawing Numbers KUO-122-203).

[9] "Technical Specifications Hope Creek Generating Station, Docket No. 50-354", U.S. Nuclear Regulatory Commission, July 1986 (NUREG-1202)

[10] Martin, G.C., "Browns Ferry Unit 3 In-Vessel Neutron Spectral Analysis," GENE, Pleasanton, CA, August 1980 (NEDO-24793).

[11] "Flux Wire Dosimeter Evaluation for the Hope Creek Generating Station," GE Report SASR 89-23, March 1989

[12] "Standard Methods for Notched Bar Impact Testing of Metallic Materials," Annual Book of ASTM Standards, E23-88

[13] "Nuclear Plant Irradiated Steel Handbook," EPRI Report NP-4797, September 1986.

[14] "Standard Methods of Tension Testing of Metallic Materials," Annual Book of ASTM Standards, E8-89.

[15] "Response To Generic Letter 92-01, Revision 1," Hope Creek Generating Station, Docket No. 50-354

[16] "Surveillance Test Specimens for Reactor Pressure Vessel," GE Number 21A8707, December 1971

[17] "Fracture Toughness Requirements," USNRC Branch Technical Position MTEB 5-2, Revision 1, July 1981.

[18] H.S. Mehta, T.A. Caine, and S.E. Plaxton, "10CFR50 Appendix G Equivalent Margin Analysis for Low Upper Shelf Energy in BWR/2 through BWR/6 Vessels," GENE, San Jose, CA, February 1994 (NEDO-32205-A, Revision 1).

APPENDIX A
CHARPY SPECIMEN FRACTURE SURFACE PHOTOGRAPHS

Photographs of each Charpy specimen fracture surface were taken per the requirements of ASTM E185-82. The pages following show the fracture surface photographs along with a summary of the Charpy test results for each irradiated specimen. The pictures are arranged in the order of base, weld, and HAZ materials.

BASE: 605
Temp: 300 °F
Energy: 133 ft-lb
MLE: 92 mils
Shear: 100 %

BASE: 613
Temp: 200 °F
Energy: 115.5 ft-lb
MLE: 81 mils
Shear: 100 %

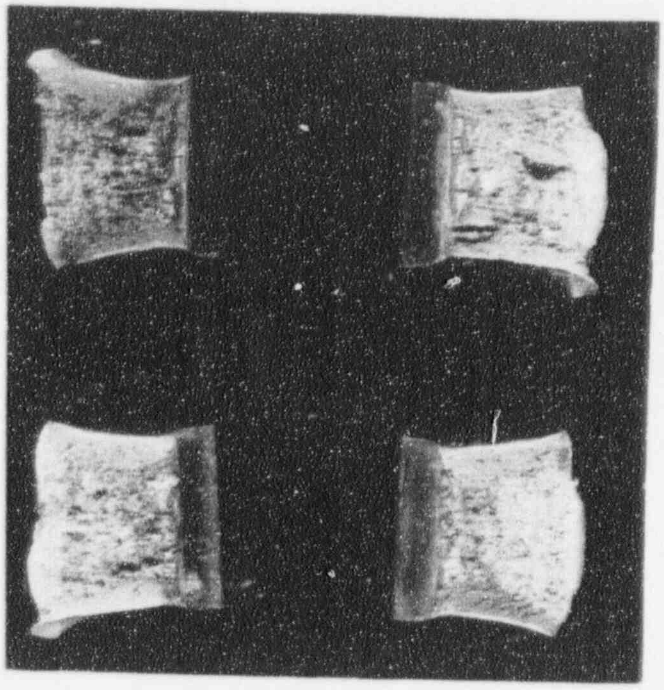

BASE: 608
Temp: 120 °F
Energy: 113.5 ft-lb
MLE: 80 mils
Shear: 100 %

BASE: 609
Temp: 80 °F
Energy: 115 ft-lb
MLE: 78 mils
Shear: 85 %

BASE: 611
Temp: 70 °F
Energy: 105 ft-lb
MLE: 84.5 mils
Shear: 79 %

BASE: 610
Temp: 60 °F
Energy: 97 ft-lb
MLE: 77 mils
Shear: 60 %

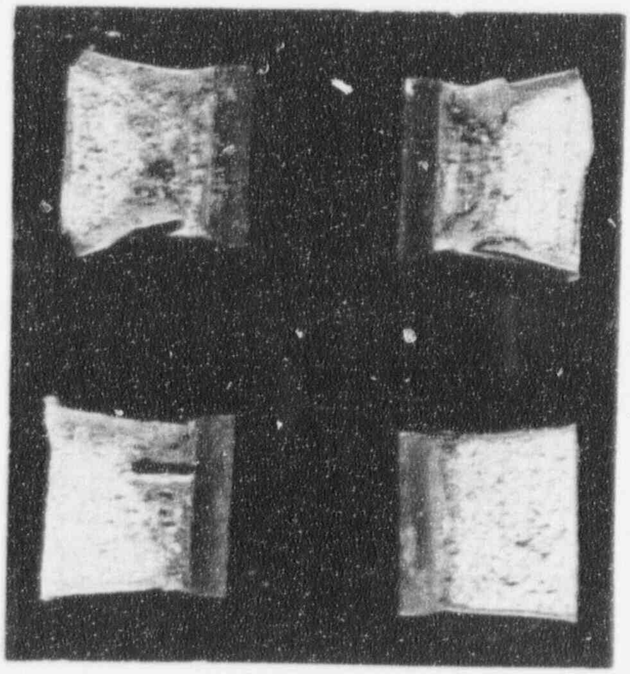

BASE: 607
Temp: 40 °F
Energy: 55 ft-lb
MLE: 50.5 mils
Shear: 52 %

BASE: 612
Temp: 0 °F
Energy: 42 ft-lb
MLE: 37 mils
Shear: 16 %

BASE: 606
Temp: -20 °F
Energy: 7 ft-lb
MLE: 8.5 mils
Shear: 18 %

BASE: 604
Temp: -50 °F
Energy: 8.5 ft-lb
MLE: 10 mils
Shear: 6 %

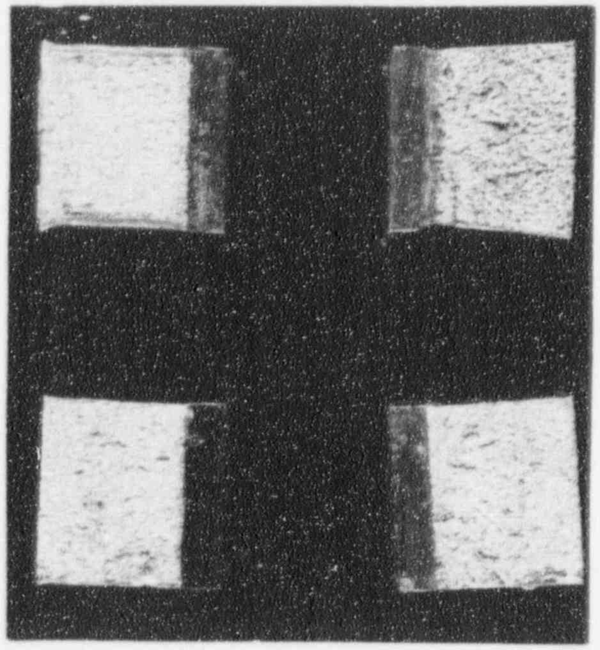

BASE: 603
Temp: -40 °F
Energy: 32.5 ft-lb
MLE: 29.9 mils
Shear: 15 %

BASE: 614
Temp: -80 °F
Energy: 7 ft-lb
MLE: 6.5 mils
Shear: 3 %

WELD: 600
Temp: 300 °F
Energy: 178.5 ft-lb
MLE: 88 mils
Shear: 100 %

WELD: 591
Temp: 150 °F
Energy: 154.5 ft-lb
MLE: 90 mils
Shear: 100 %

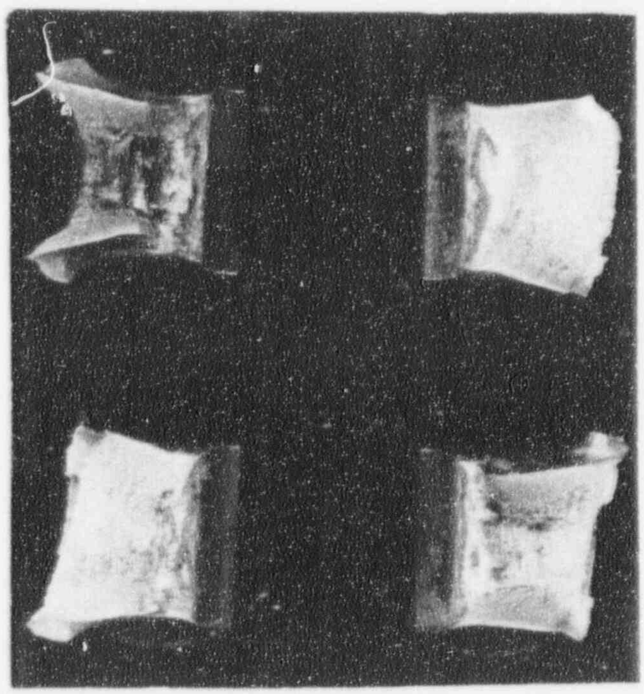

WELD: 602
Temp: 200 °F
Energy: 144.5 ft-lb
MLE: 91 mils
Shear: 100 %

WELD: 598
Temp: 120 °F
Energy: 147.5 ft-lb
MLE: 92 mils
Shear: 100 %

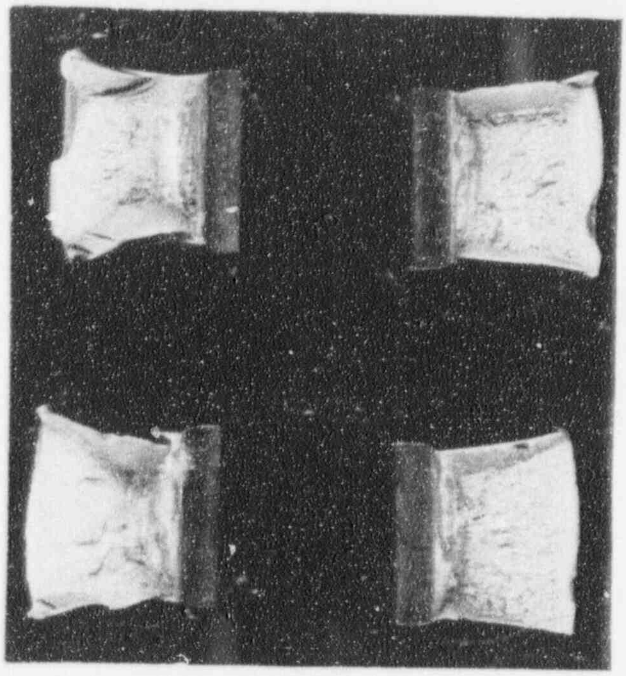

WELD: 593
Temp: 80 °F
Energy: 112.5 ft-lb
MLE: 69 mils
Shear: 77 %

WELD: 601
Temp: 50 °F
Energy: 61 ft-lb
MLE: 44 mils
Shear: 58 %

WELD: 599
Temp: 40 °F
Energy: 88.5 ft-lb
MLE: 72 mils
Shear: 50 %

WELD: 596
Temp: 20 °F
Energy: 59.5 ft-lb
MLE: 48.5 mils
Shear: 39 %

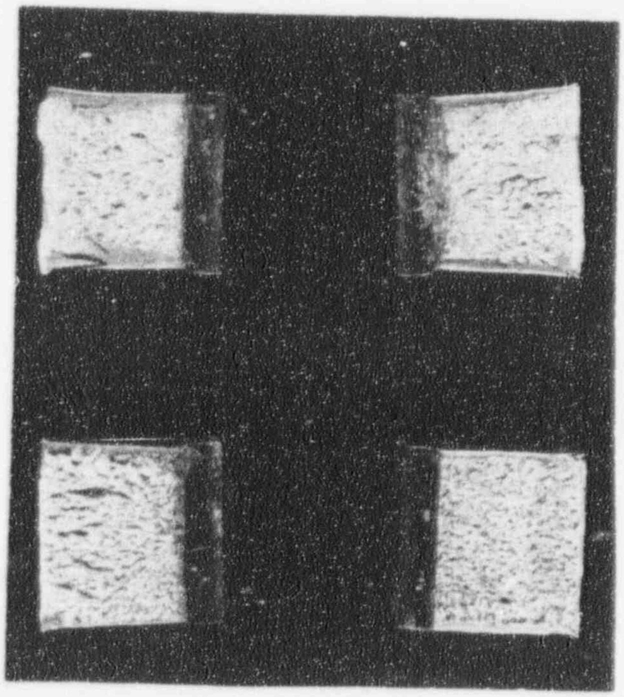

WELD: 592
Temp: 0 °F
Energy: 19.5 ft-lb
MLE: 22.5 mils
Shear: 34 %

WELD: 595
Temp: -10 °F
Energy: 31 ft-lb
MLE: 27 mils
Shear: 26 %

WELD: 597
Temp: -40 °F
Energy: 22.5 ft-lb
MLE: 20 mils
Shear: 17 %

WELD: 594
Temp: -80 °F
Energy: 5.5 ft-lb
MLE: 9.5 mils
Shear: 12 %

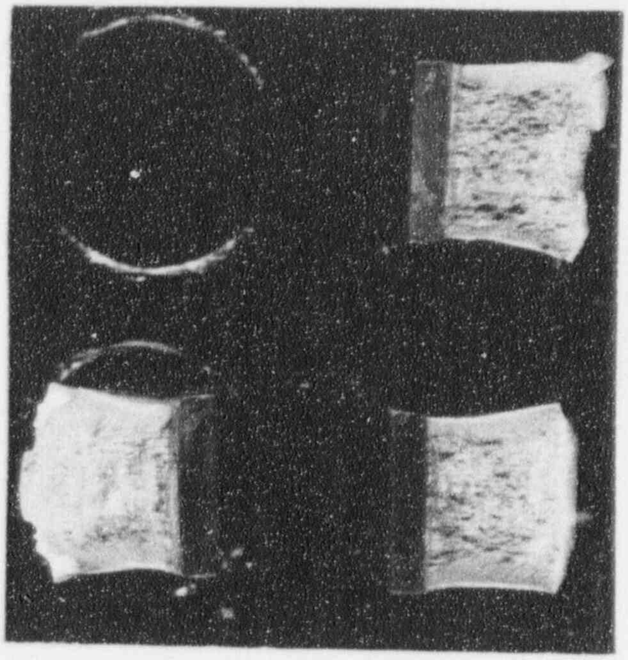

HAZ: 625
Temp: 200 °F
Energy: 85 ft-lb
MLE: 68 mils
Shear: 100 %

HAZ: 615
Temp: 150 °F
Energy: 172.5 ft-lb
MLE: 78 mils
Shear: 100 %

HAZ: 620
Temp: 120 °F
Energy: 80.5 ft-lb
MLE: 59 mils
Shear: 100 %

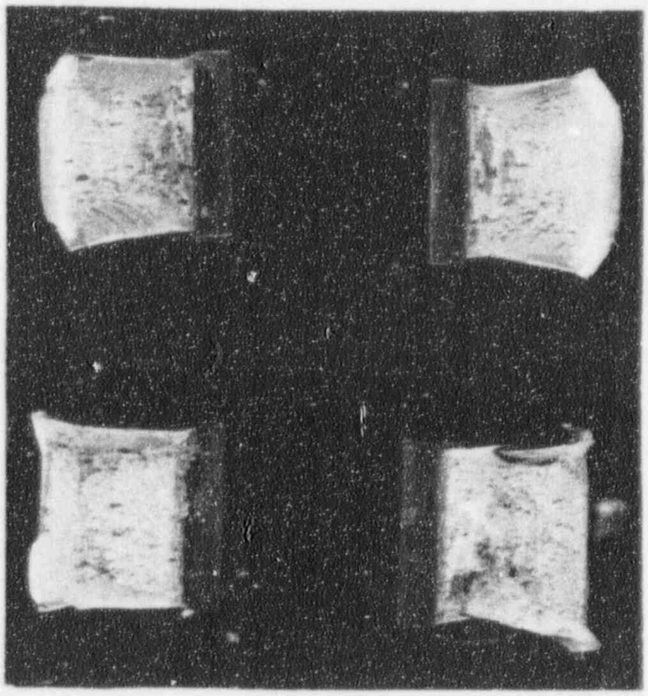

HAZ: 617
Temp: 80 °F
Energy: 112.5 ft-lb
MLE: 75 mils
Shear: 92 %

HAZ: 618
Temp: 70 °F
Energy: 153 ft-lb
MLE: 84 mils
Shear: 100 %

HAZ: 621
Temp: 40 °F
Energy: 41 ft-lb
MLE: 34 mils
Shear: 41 %

HAZ: 622
Temp: 0 °F
Energy: 128.5 ft-lb
MLE: 79 mils
Shear: 79 %

HAZ: 623
Temp: -10 °F
Energy: 59 ft-lb
MLE: 41 mils
Shear: 43 %

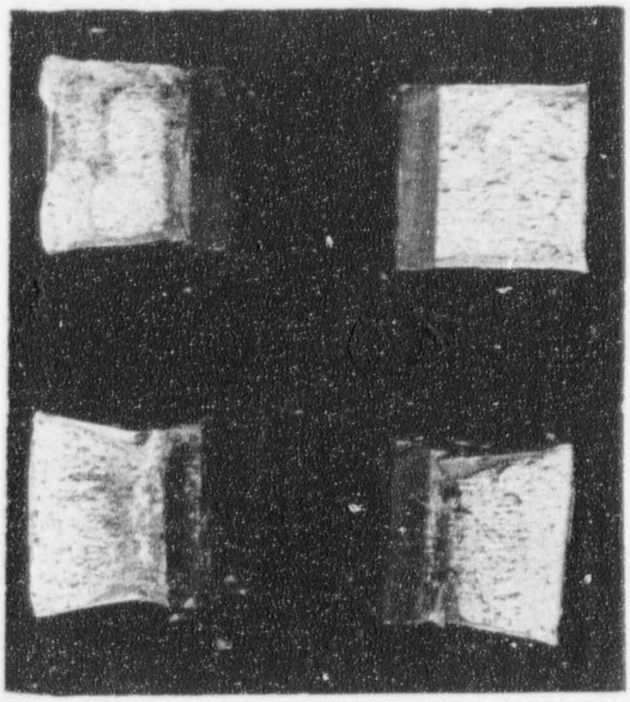

HAZ: 626
Temp: -40 °F
Energy: 9.5ft-lb
MLE: 10 mils
Shear: 26 %

HAZ: 624
Temp: -80 °F
Energy: 85 ft-lb
MLE: 59 mils
Shear: 44 %

HAZ: 616
Temp: -100 °F
Energy: 70 ft-lb
MLE: 48 mils
Shear: 33 %

HAZ: 619
Temp: 300 °F
Energy: >233 ft-lb
MLE: 61 mils
Shear: 100 %

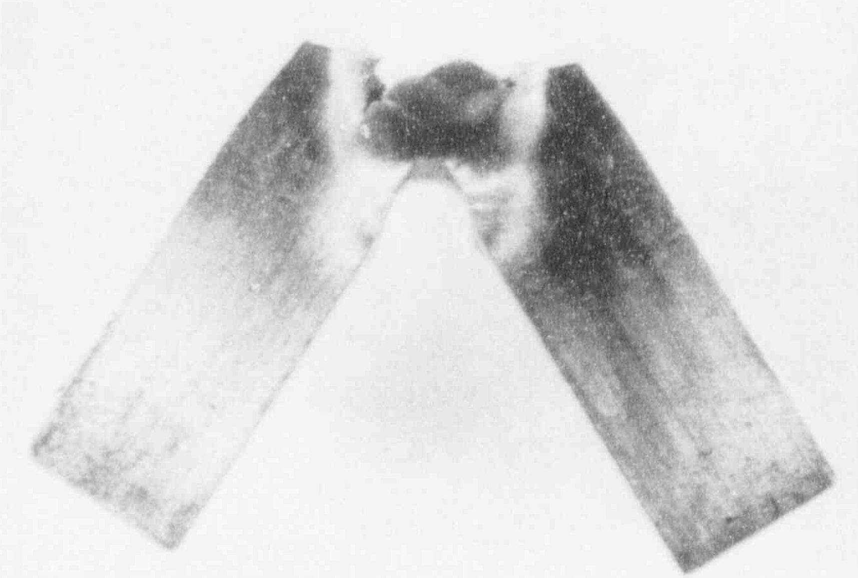

APPENDIX B
EQUIVALENT MARGIN ANALYSIS

TABLE B-1
EQUIVALENT MARGIN ANALYSIS
PLANT APPLICABILITY VERIFICATION FORM
FOR HOPE CREEK UNIT 1 - BWR 4/MK I

BWR/3-6 PLATE

Surveillance Plate USE:

%Cu = 0.09

Capsule Fluence = 1.42×10^{17} n/cm^2

Measured % Decrease = 14 (Charpy Curves)

R.G. 1.99 Predicted % Decrease = 7 (R.G. 1.99, Figure 2)

Limiting Beltline Plate USE:

%Cu = 0.15

32 EFPY 1/4-T Fluence = 5.2×10^{17} n/cm^2

R.G. 1.99 Predicted % Decrease = 12 (R.G. 1.99, Figure 2)

Adjusted % Decrease = 19 (R.G. 1.99, Position 2.2)

19 % ≤ 21%, so vessel plates are bounded by equivalent margin analysis

TABLE B-2
EQUIVALENT MARGIN ANALYSIS
PLANT APPLICABILITY VERIFICATION FORM
FOR HOPE CREEK UNIT 1 - BWR 4/MK I

BWR/2-6 WELD

Surveillance Weld USE:

%Cu = 0.08

Capsule Fluence = 1.42×10^{17} n/cm^2

Measured % Decrease = 5 (Charpy Curves)

R.G. 1.99 Predicted % Decrease = 8.5 (R.G. 1.99, Figure 2)

Limiting Beltline Weld USE:

%Cu = 0.10

32 EFPY Fluence = 5.2×10^{17} n/cm^2

R.G. 1.99 Predicted % Decrease =12 (R.G. 1.99, Figure 2)

Adjusted % Decrease = N/A (R.G. 1.99, Position 2.2)

12 % ≤ 34%, so vessel welds are bounded by equivalent margin analysis